

**Adsorption-supported ozonation of complex mariculture wastewater pharmaceuticals by greener (Ni/Fe-C) nano-composite derived by co-pyrolysis of Coconut Shell & partially reduced iron: mechanism, and implications**

Muhammad Noman <sup>a, b</sup>, Guangwei Yu\* <sup>a</sup>

<sup>a</sup> State Key Laboratory of Advanced Environmental Technology, Institute of Urban Environment, Chinese Academy of Sciences, Xiamen, Fujian 361021, China

<sup>b</sup> University of Chinese Academy of Sciences, Beijing 100049, China

\* Corresponding author.

E-mail address: [gwyu@iue.ac.cn](mailto:gwyu@iue.ac.cn) (Guangwei Yu)

### **Text S1. Chemicals, materials, and nano-composites synthesis**

Oxytetracycline ( $C_{22}H_{24}N_2O_9$ ) (79-57-2)  $\geq 99\%$ , HPLC was purchased from Aladdin Macklin Biochemical Co., Ltd. (Shanghai, China). Coconut shell residues were obtained after food waste at a plant at the Xiamen Eastern Solid Waste Treatment Center. Partially reducing iron ore waste was collected from pig iron manufacturing units. Dimethyl sulfoxide ( $C_2H_6OS$  F.W. 78.13,  $\geq 99.5\%$ ), tert-butanol ( $C_4H_{10}O$  F.W. 74.12  $\geq 99.5\%$ ), 2,2,6,6-tetramethylpiperidine (TEMP,  $\geq 98.0\%$ ), and 5 5-dimethyl-1-pyrroline-N-oxide (DMPO,  $\geq 97.0\%$ ) were purchased from Shanghai Maclean's Biochemical Technology Co., Ltd. In addition, 1-4 Benzoquinone (BQ  $\geq 97.0\%$ ) was purchased from Tokyo Chemical Industry Co., Ltd. Sodium chloride NaCl (F.W. 58.44,  $\geq 99.5\%$ ). All chemical reagents employed in this study were analytically pure. Super deionized water (SDI) was used in a Milli-Q Biocel water system, and the oven was purchased from Shanghai Jinghong Experimental Equipment Co., Ltd. All pieces of glassware were washed with SDI water several times before being used and then dried in an oven at 105 °C.

**Nano-composite Synthesis:** Co-pyrolysis was carried out in a horizontal tube furnace (OTF-1200X, MTI Corp.) with a 60 mm O.D. quartz tube. A 5 g portion of the Coconut shell residue (CNR) and 1 g reduced iron (RI) powder (5:1 w/w) was spread as a thin layer (ca. 1 mm) on a quartz boat and placed in the constant temperature zone of the tube. The samples were heated from room temperature to 300-700 °C at 5 °C  $min^{-1}$  under flowing  $N_2$  (200 mL  $min^{-1}$ , 99.99 % purity). The temperature was held for 45 min, then the furnace was shut off and allowed to cool naturally to below 60 °C under flowing  $N_2$  (200 mL  $min^{-1}$ ). Targets of 300 °C and 500 °C were run with the same heating rate, hold time, and gas flow.

### **Reproducibility:**

The entire 300-700 °C run was repeated three times (on different days, using different 5 g of CNR and 1 g of RI scoops from the well-mixed stock) to demonstrate reproducibility, with the following results (mean  $\pm$  uncertainty): solid yield  $30.2 \pm 1.4$  % and Fe content  $10.1 \pm 0.2$  wt % (ICP-OES). Bed temperature was within  $\pm 3$  °C of 300-700 °C for all three runs, N<sub>2</sub> flow drift was  $< 1$  %, and outlet O<sub>2</sub> was  $< 10$  ppm.

---

Run ID	Solid yield (%)	Fe (wt%)
R-700-1	25.3	16.4
R-700-2	24.8	16.2
R-700-3	25.2	16.3
Mean $\pm$ SD	$25.1 \pm 0.3$	$16.3 \pm 0.1$

\*yield = (final mass / 6 g)  $\times 100$  %.

### **Text S2: Catalytic Characterization and Analytical Method**

The physiological morphology and elemental composition of all SCS@BR catalysts were examined using advanced technologies, including Energy Dispersive Spectroscopy (E.D.S.), Scanning electron microscopy (S.E.M., S-4800, Hitachi, Japan), and a transmission electron microscope (T.E.M., JEM1200EX, J.E.O.L., Japan). ASAP 2020. X-ray photoelectron spectroscopy (XPS) was used to analyze the chemical environment before and after the reaction. The instrument used for this analysis was the Axis Supra XPS and X-ray Fluorescence Spectrometer system manufactured by Shimadzu in Japan. To know about the TOC values, catalytically degraded samples were analyzed by a TOC analyzer (TOC—LCPH, Shimadzu,

Japan). COD values of all samples were determined by utilizing COD (HJ/T 399-2007) with an automatic digester by Shandong Horde Electronic Technology Co., Ltd. A ball mill (XQM-4; Changsha Tian-chuang Power Technology, China) was used.

The total organic elimination efficiency following the reaction was measured using a T.O.C. (Japanese Shimadzu) instrument. In addition, identifying potential reactive oxygen species (R.O.S.) created for mechanism research was conducted utilizing a Bruker Electron Spin Resonance spectrometer (ESR). A powder diffraction meter (XRD, X 'Pert Pro, P.A.N. analytical, Netherlands) was equipped with Cu-K $\alpha$  radiation ( $\lambda = 1.5444426 \text{ \AA}$ ) to determine the crystallinity of the Fe-BRB modified. Fourier transform infrared spectroscopy (FT-IR) was conducted using the KBr pellet technique over 4000 to 400  $\text{cm}^{-1}$ . LC-MS was used to determine the OFL intermediate products throughout the catalytic degradation reaction, thereby uncovering the potential pathway of OFL degradation.

### **Analytical methods:**

**Catalytic activity calculations:** The following equations calculate the degradation efficiency/catalytic activity of OTC

$$\text{Degradation efficiency of OTC (\%)} = \left[ \frac{C_t - C_o}{C_o} \right] \times 100\% \quad (1)$$

$C_t$  is the concentration at a particular time (min), and  $C_o$  is the initial concentration of OTC. COD is the value of the chemical oxygen demand at time ( $t=0$ ) and time ( $t$ ) of all samples.

$$\text{Degradation efficiency of COD (\%)} = \left[ \frac{COD_t - COD_o}{COD_o} \right] \times 100\% \quad (2)$$

All optimized catalytic ozonation degradation experiments were performed and repeated, and then the average values were taken. Additionally, standard deviation (SD) values

for OTC over SDI water and stimulated urine experimental values were taken for repeated experimental values.

$$SD_{mean} = \sqrt{\frac{SD_1^2 + SD_2^2}{2}} \quad (3)$$

$SD_1^2$  and  $SD_2^2$  It is the standard deviation of repeated experiments.

Further, standard error (SE) values were also calculated using the following values. “n” represents the number of samples taken over 100 min of catalytic reaction.

$$SE = \frac{SD}{\sqrt{n}} \quad (4)$$

All DFT work was carried out in **Materials Studio 2020** with the **DMol<sup>3</sup>** module. We chose the **PBE GGA** functional plus the **TS dispersion correction** to capture long-range forces, used the numerical double- $\zeta$  **polarized DNP 4.4** basis set within a **3.5 Å** cutoff, and kept **core electrons frozen** with the **DFT semi-core pseudopotential**. The model was a single-layer graphene flake whose zig-zag edge carried one substitutional Ni or Fe atom; a **15 Å** vacuum slab prevented periodic images. Optimizations converged to forces below **0.004 Ha Å<sup>-1</sup>** and energy changes below **1 × 10<sup>-5</sup> Ha**. Ozone was docked side-on to the metal–carbon bond, and reaction paths were traced with the **LST/QST algorithm**, each transition-state verified by one imaginary frequency; spin polarization was retained throughout.

**Text. S3: Escherichia coli (E. coli) growth, Chinese cabbage growth, and Zebra-fish embryo assessment over SDI, polluted and treated wastewater samples**

**Chinese cabbage grain growth:** For the germination of the Chinese cabbage, healthy grains were put into three different plates having SDI, contaminated water, and treated water after cleaning and washing, for 80 days, and the temperature was maintained at 30°C.

**Escherichia coli (E. coli) growth:**

**Materials Required:**

All solutions were prepared using SDI water. The Luria Bertani (LB) broth was made by dissolving 10 g of LB powder in 500 mL of water. A saline solution was prepared by dissolving 20 g of NaCl per liter of water. Agar-agar powder (8 g) was added to 500 mL of LB broth to create solid LB agar media. For the buffer solution, sodium dihydrogen phosphate ( $\text{NaH}_2\text{PO}_4$ ) and disodium phosphate ( $\text{Na}_2\text{HPO}_4$ ) were used in a 1:1 ratio. The equipment used included an incubator, a Bunsen burner or alcohol lamp (for sterilizing inoculating loops), and an *E. coli* bacterial culture.

### **Preparation of Solid Media Plates:**

*Escherichia coli* was cultured by inoculating a known working stock into LB liquid medium and incubating at 30 °C for 12 h. The culture was centrifuged at 8,000 rpm for 10 min, the supernatant removed, and the pellet resuspended in sterile buffer to an  $\text{OD}_{600}$  of 2. Agar plates were made by dissolving the medium, autoclaving at 121 °C for 30 min, cooling to 50 °C, and pouring aseptically into sterile Petri dishes. For enumeration, serial dilutions were made in PBS (eight-fold,  $10^{-1}$  to  $10^{-8}$ ) by transferring 1  $\mu\text{L}$  of culture into 9  $\mu\text{L}$  of sterile PBS, mixing well, and plating 0.1 mL of each dilution onto the agar. After incubation at 37 °C for 24 h, colonies were counted before and after antibiotic exposure to determine treatment efficacy. In parallel phytotoxicity tests, agricultural soil was sown with 5 g of wheat grains and irrigated for 5 days with (i) sterile distilled water (SDI), (ii) raw mariculture wastewater, (iii) untreated wastewater, and (iv) ozonation-treated wastewater; significant differences in germination and shoot length were noted.

### **Zebra fish embryo growth:**

Zebrafish embryos, collected within 2 hours post-fertilization (hpf), were maintained in E3

medium at 28 °C. At 24 hpf, enzymatic dechorionation was performed using pronase, followed by anaesthesia with 0.02 mg ml<sup>-1</sup> tricaine at 48 hpf. Subsequently, the embryos were divided into three distinct treatment groups: (i) ozonation-treated mariculture water, (ii) untreated mariculture water, and (iii) sterile distilled water (SDI). Incubation proceeded at 28 °C, with observations conducted every 24 hours. At 120 hpf, key parameters including hatching success, heart rate, axial curvature, and total length were documented and statistically compared across the treatments, ensuring compliance with an approved ethical protocol.

#### **Test S4. Avoided Burdens from Waste Utilization (Waste-Based Catalyst Preparation)**

##### **Avoided-burden equation (waste-based catalyst)**

Avoided Impact<sub>i</sub> [kg CO<sub>2</sub>-eq or PO<sub>4</sub>-eq] = m\_waste [kg] × CF\_disposal,i [kg\_waste<sup>-1</sup> kg CO<sub>2</sub>-eq] [1] , [2]

##### **Description**

- *m<sub>waste</sub>*: mass of coconut-shell residue or partially-reduced iron ore waste diverted from disposal and used in the composite (kg).
- CF<sub>disposal,i</sub>: characterization factor for the avoided disposal route (landfill, incineration, etc.) and impact category *i* (GWP, eutrophication, etc.).
- Product of the two terms quantifies the environmental credit gained by not landfilling or incinerating the waste.

#### **2. Toxicity from Potential Impurities in Waste Feedstock (Catalyst Preparation & Usage)**

##### **Toxicity-impact equation (impurities from waste feedstock)**

$$\text{Impact}_{\text{toxicity},j} [\text{CTUh}] = k \sum m_{\text{toxic},k} [\text{kg}] \times \text{CF}_{\text{toxicity},j,k} [\text{kgCTUh}]$$

[3] [4]

### What each term means

- $Impact$  – total toxicity score for category  $j$  (human toxicity, freshwater ecotoxicity, etc.).
- $m$  – mass of impurity  $k$  (heavy metal, POP, etc.) released during catalyst preparation or use.
- $CF$  – characterization factor that converts kilograms of substance  $k$  into comparative toxic units (CTU), accounting for fate, exposure, and effect.

### 3. Resource Efficiency & Circularity Metrics (Catalyst Life Cycle)

**Material Circularity Indicator (MCI)** – Ellen MacArthur Foundation [5], [6], [7].

$$MCI = (1 - V) \times ((1 - F_m) / (F_w + F_c))$$

**Table**

Symbol	Meaning (fraction or ratio)
V	Virgin material input per functional unit (kg virgin/kg product)
F <sub>m</sub>	Share of <b>recycled material</b> in the <b>feedstock</b> (mass%)
F <sub>w</sub>	Share of <b>virgin material</b> in the <b>feedstock</b> (mass%)
F <sub>c</sub>	Share of <b>recycled content</b> in the <b>final product</b> (mass%)

**Interpretation:**

$MCI = 1 \rightarrow \text{perfect circularity}$  (no virgin input, fully recycled).

$MCI = 0 \rightarrow \text{linear system}$  (all virgin, no recycling).

#### 4. Regeneration Efficiency and Impact (Catalyst Discharge/End-of-Life)

##### Regeneration credit per functional cycle

Credit reg,  $i$  [Cycle kg CO<sub>2</sub>-eq] = (Impact fresh,  $I$  – Impact reg,  $i$ ) $\times$ Number of Cycles

[8]

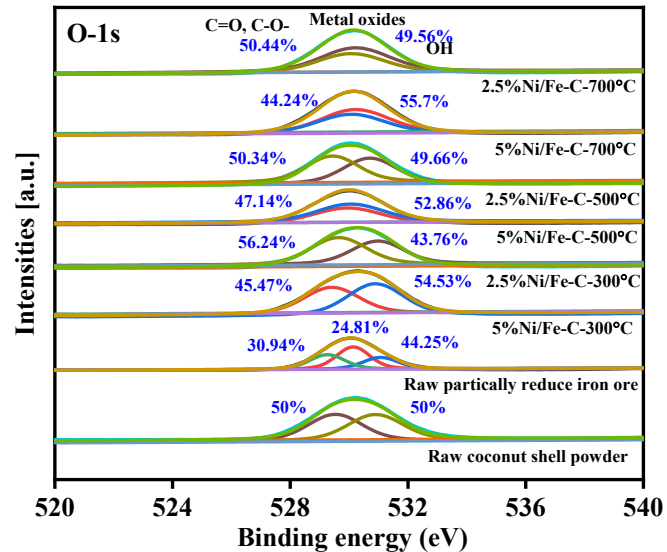
Term	Meaning
<b>Impact<sub>fresh</sub></b>	Life-cycle impact of producing a <b>virgin</b> catalyst for category $i$ (e.g., GWP, CO <sub>2</sub> -eq).
<b>Impact<sub>reg</sub></b>	Life-cycle impact of <b>one regeneration</b> cycle (energy, chemicals, emissions) for the same category.
<b>Number of Cycles</b>	Completed regeneration loops before catalyst discard.

##### Interpretation:

The equation quantifies the **net environmental saving** obtained by regenerating the waste-derived catalyst instead of repeatedly manufacturing fresh material.

Figure S1: O-1s peaks of all bimetallic (Fe/Ni) nano-composites

(a)



(b)

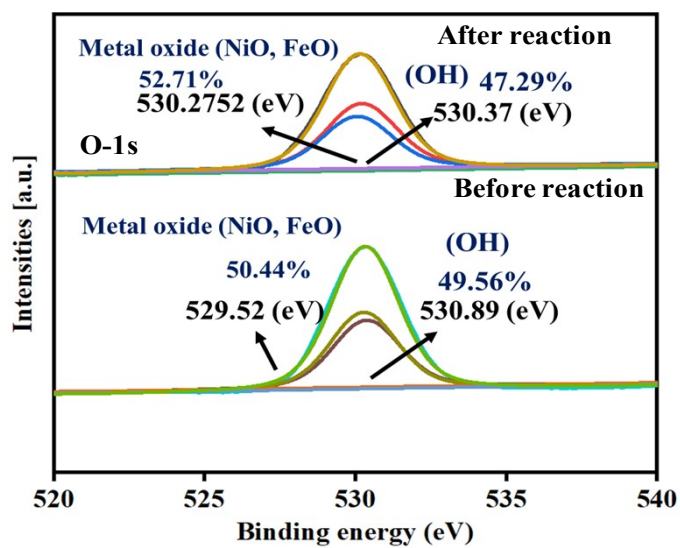


Figure S2: 3D-EEMs OTC treatment before and after reaction

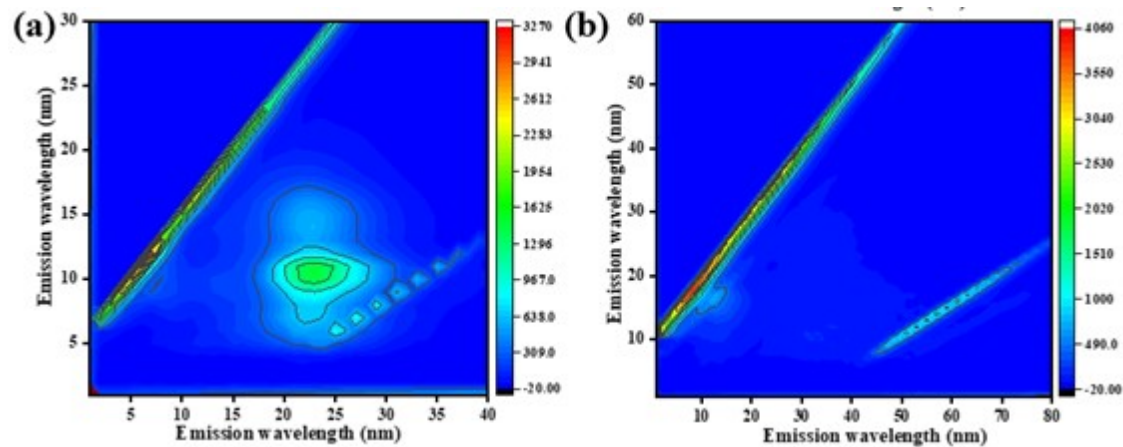
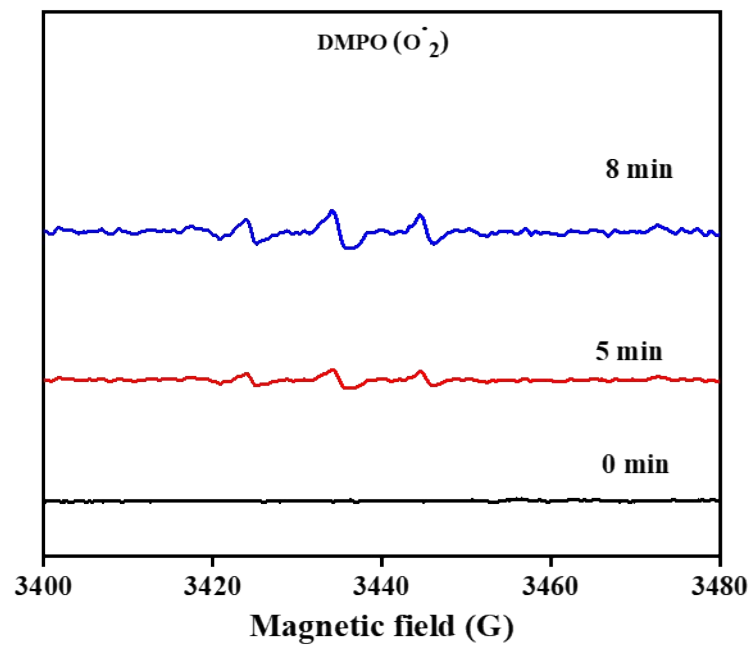
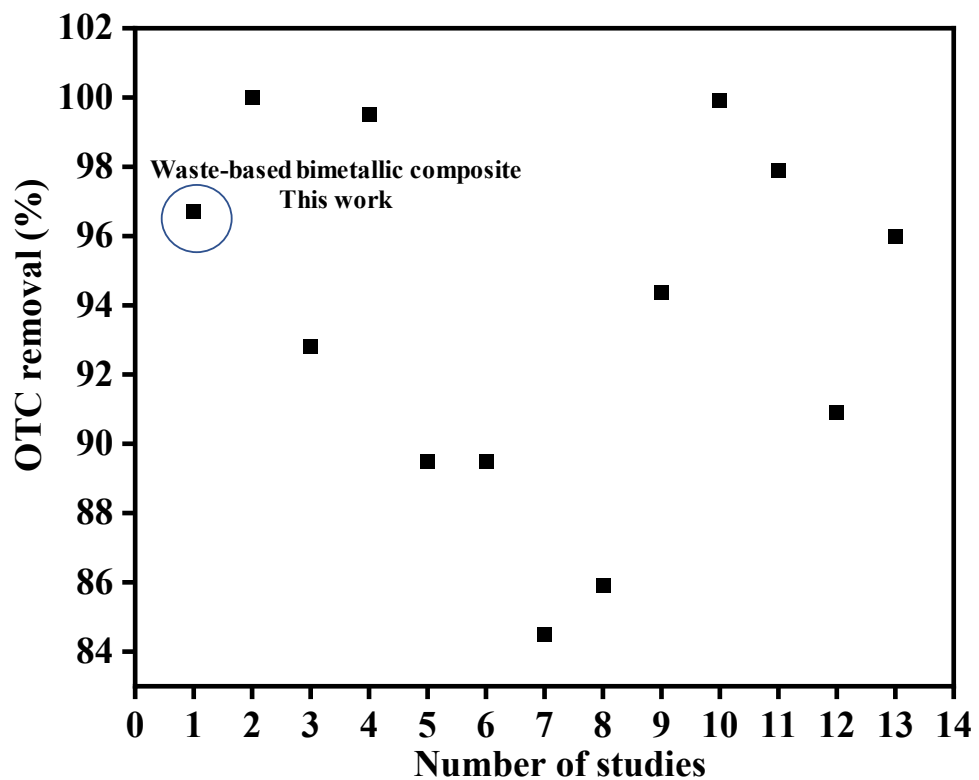


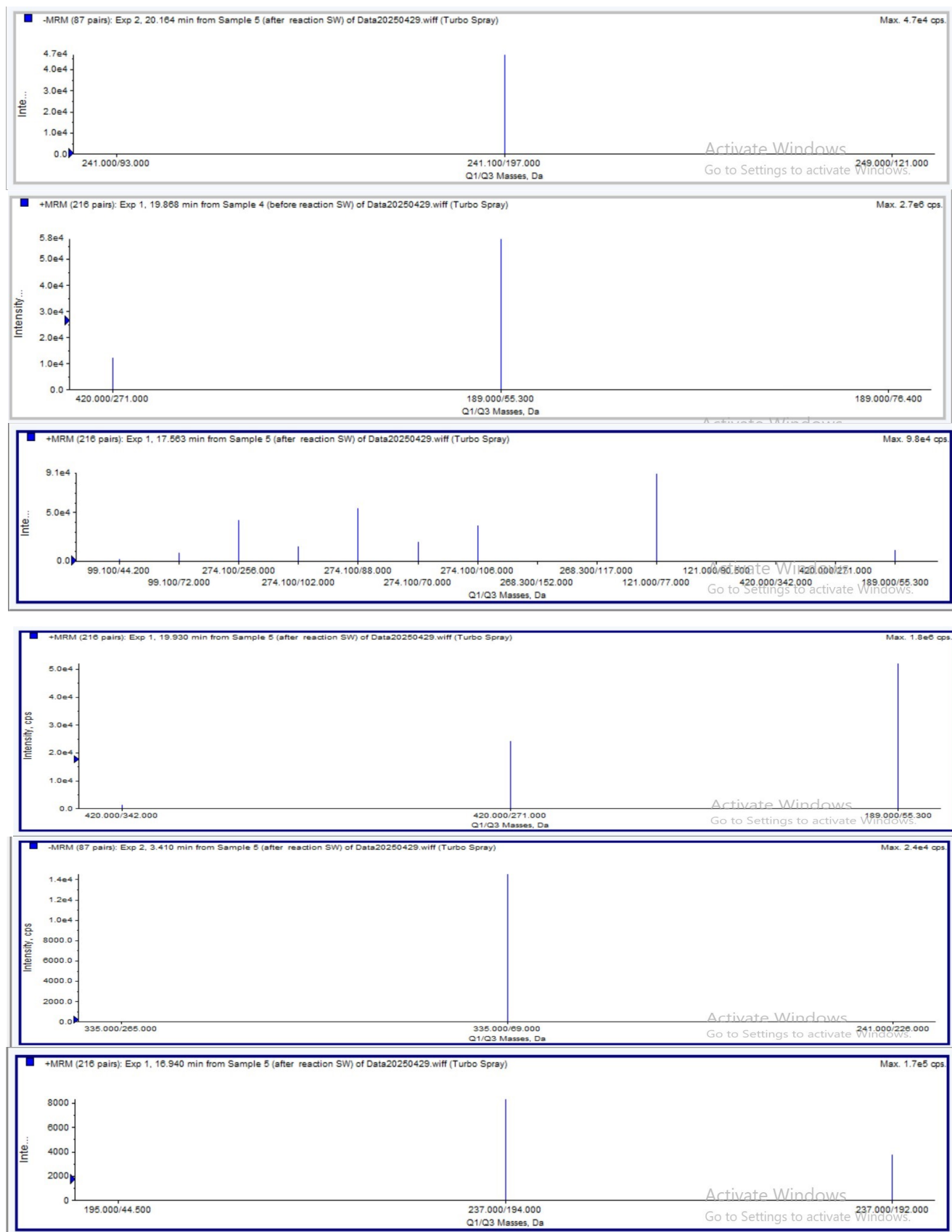
Figure S3: DMPO singles trapped superoxide radicals ( $O_2^{\cdot-}$ )

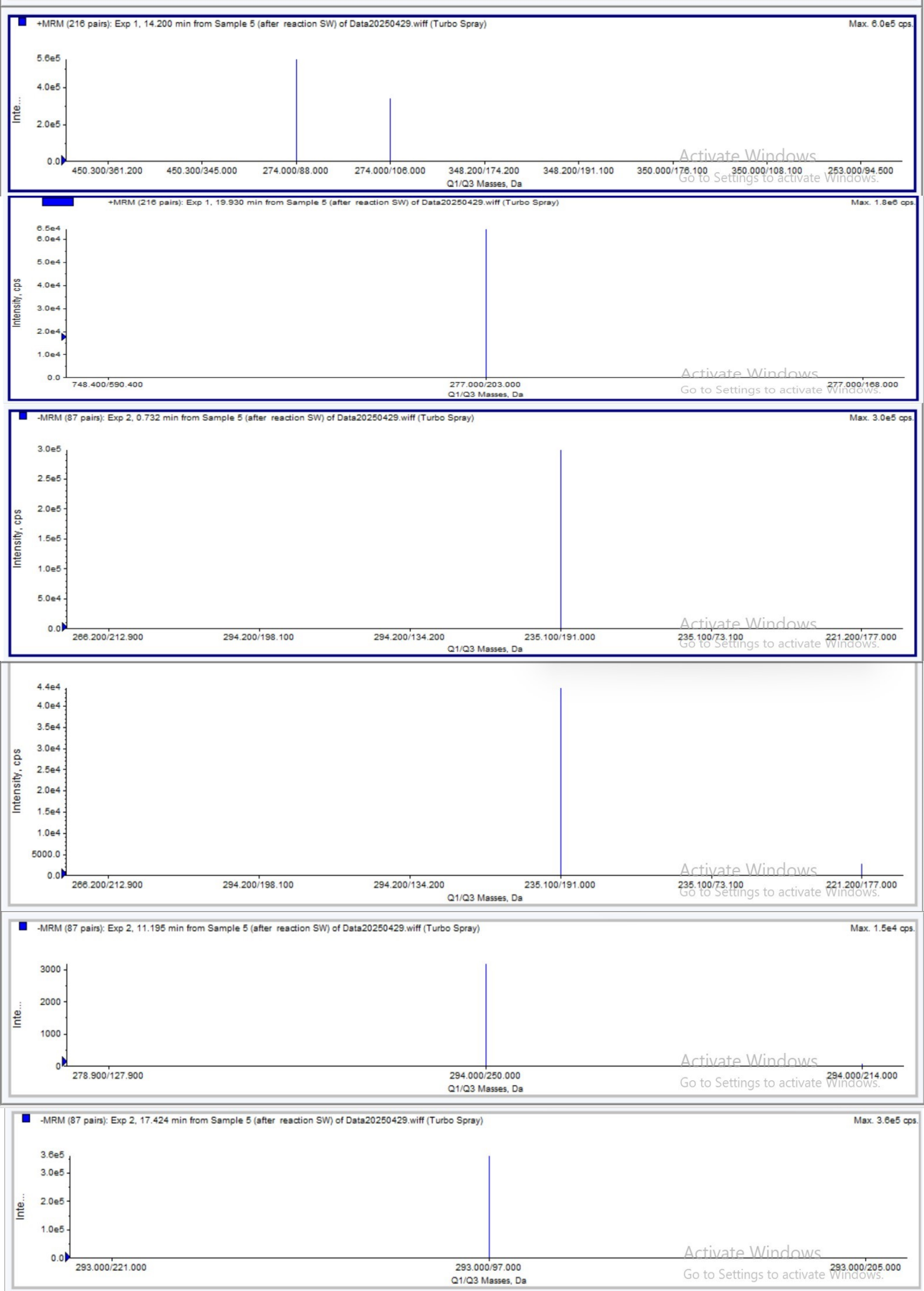


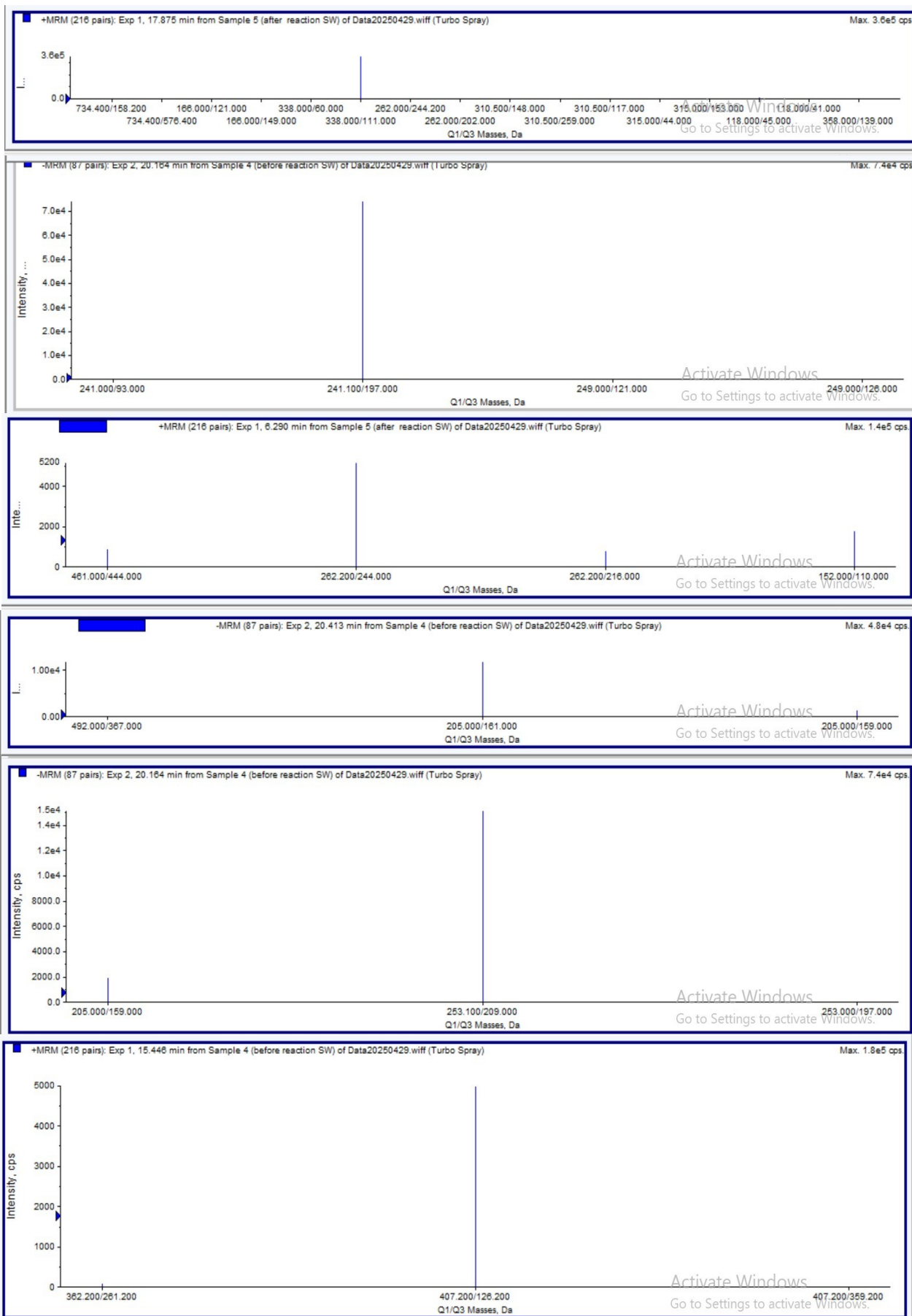
**Figure S4: Performance comparison**

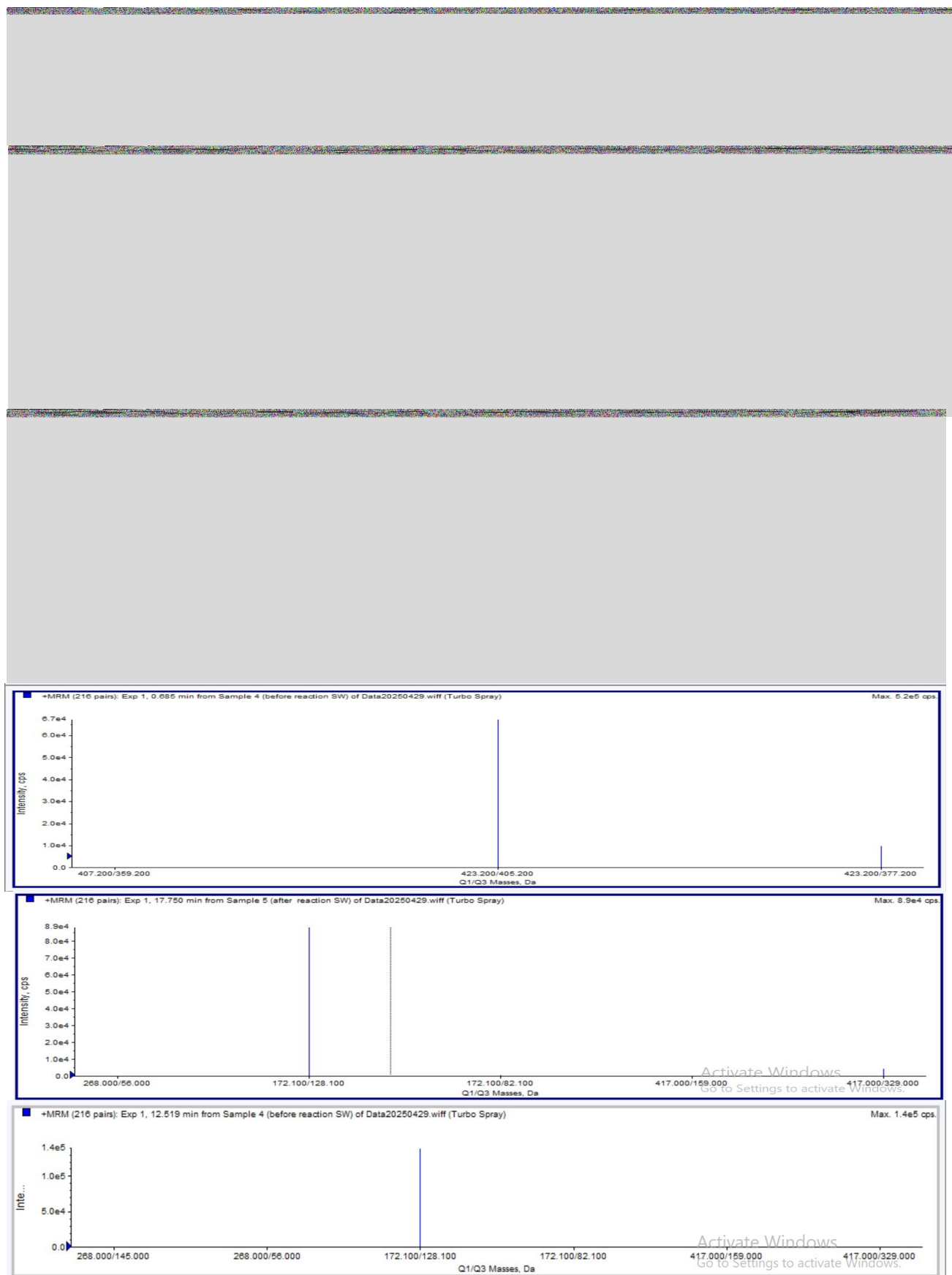


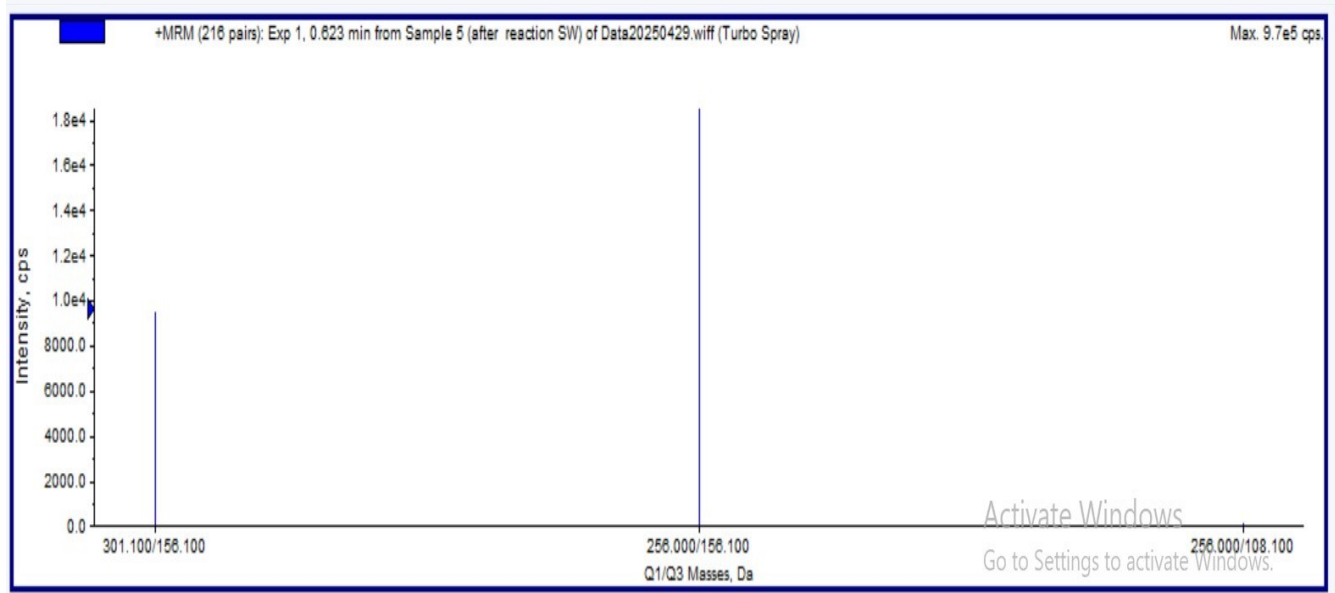
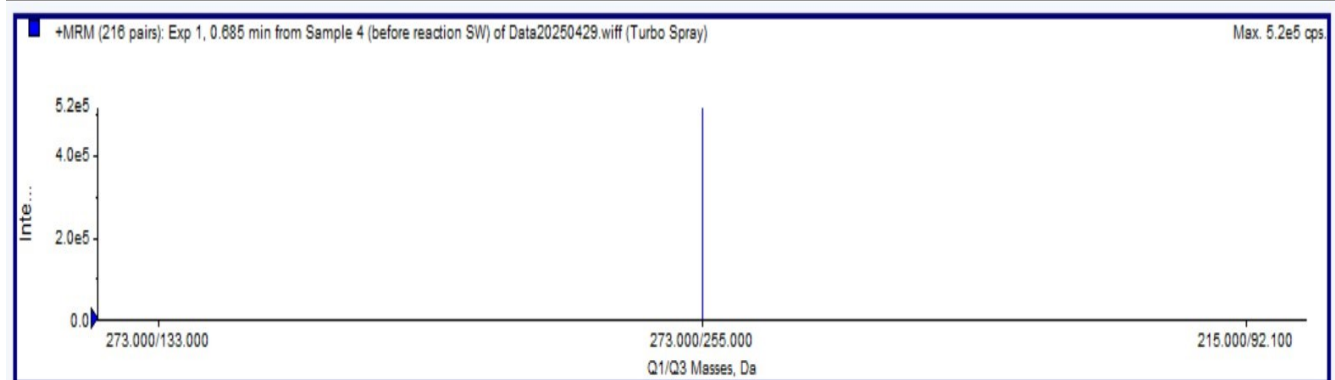
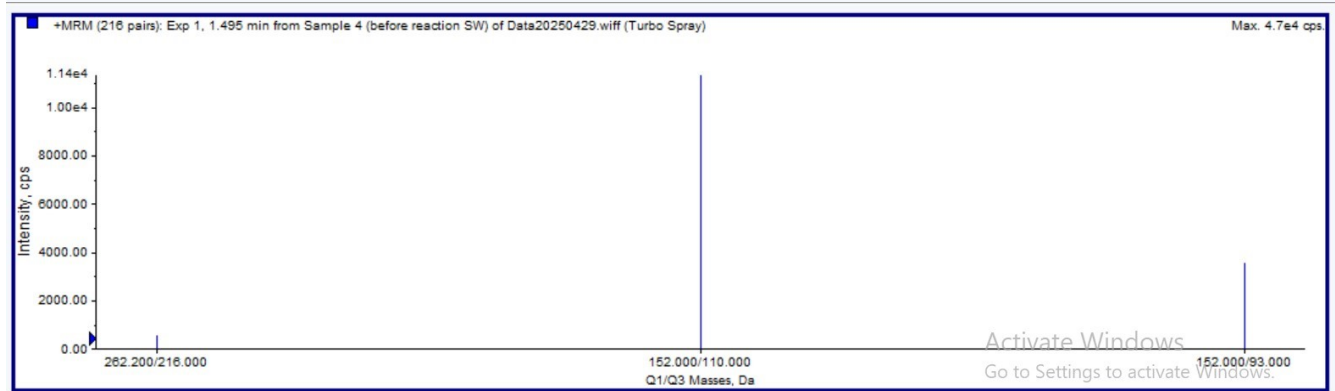
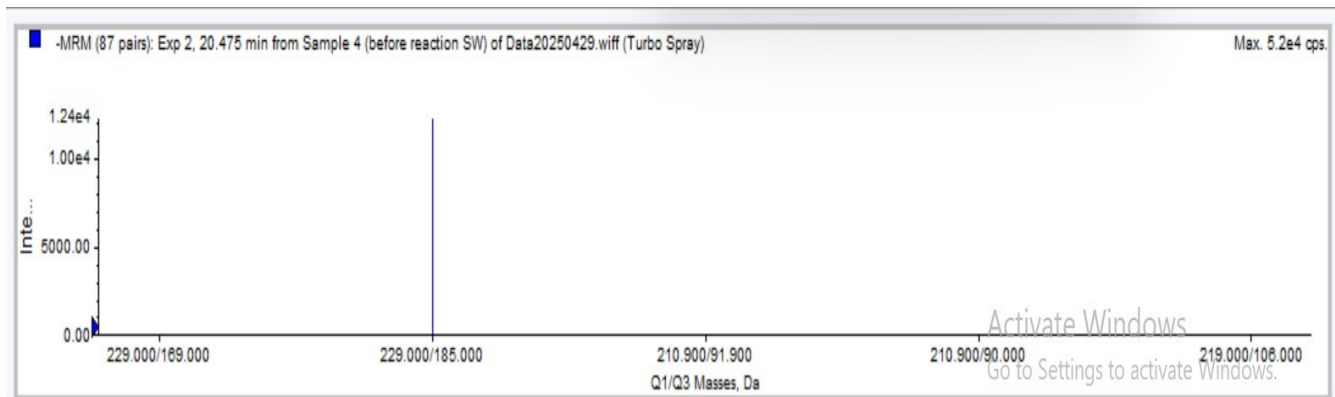
**Figure S5: Mariculture wastewater toxic pharmaceuticals (Before reaction)**



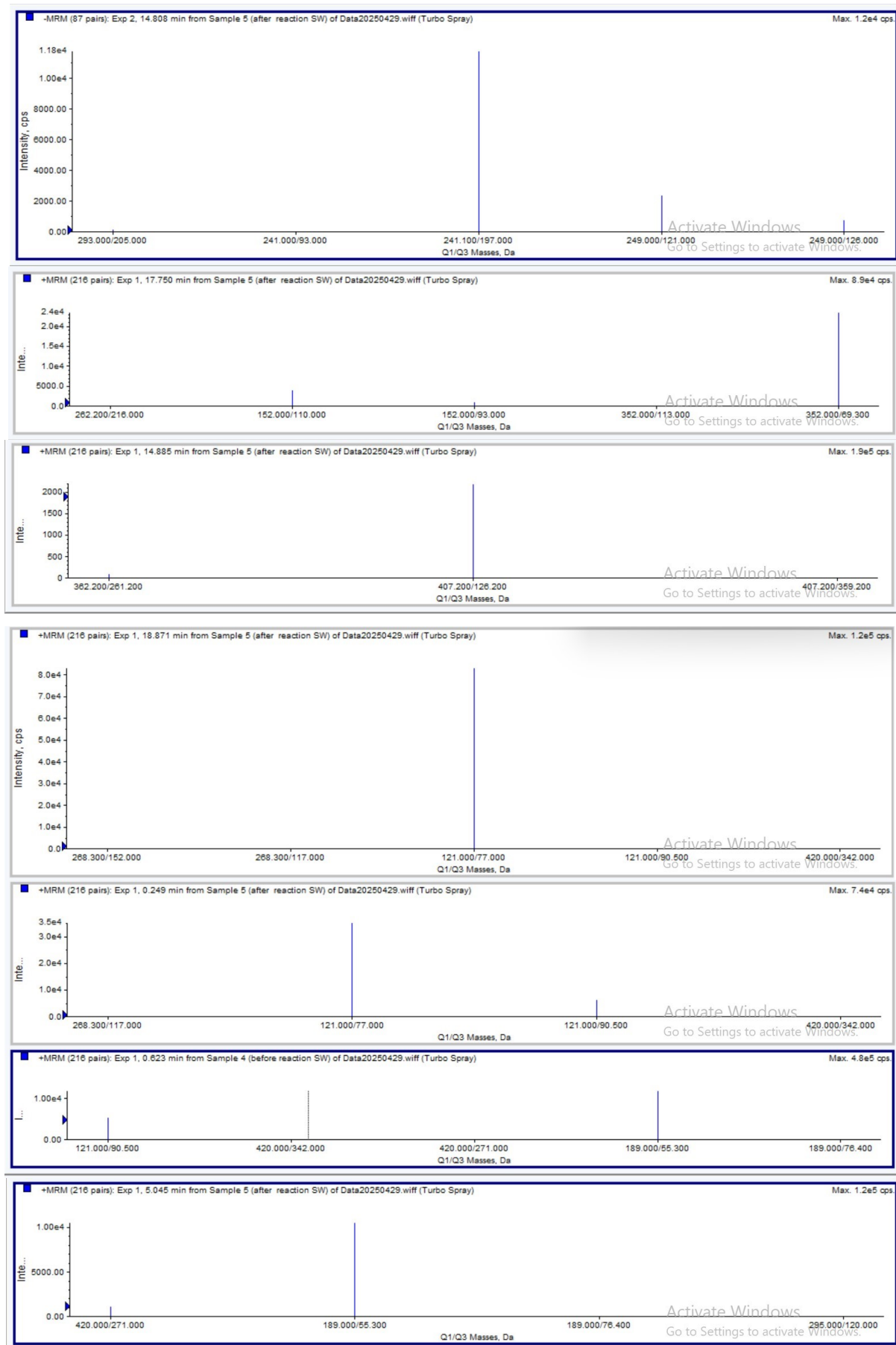


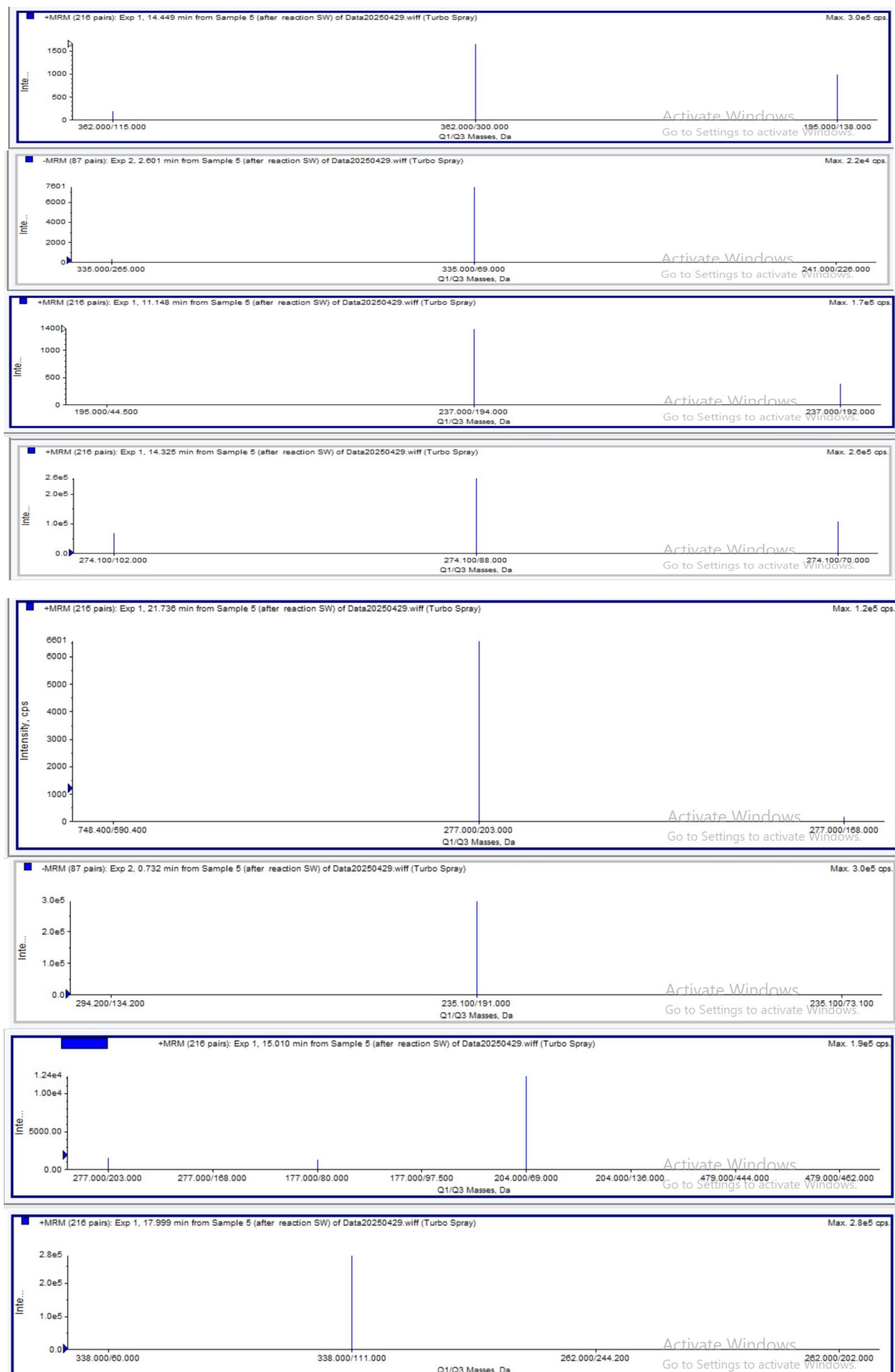






**Figure S6: Mariculture wastewater toxic pharmaceuticals (After reaction)**





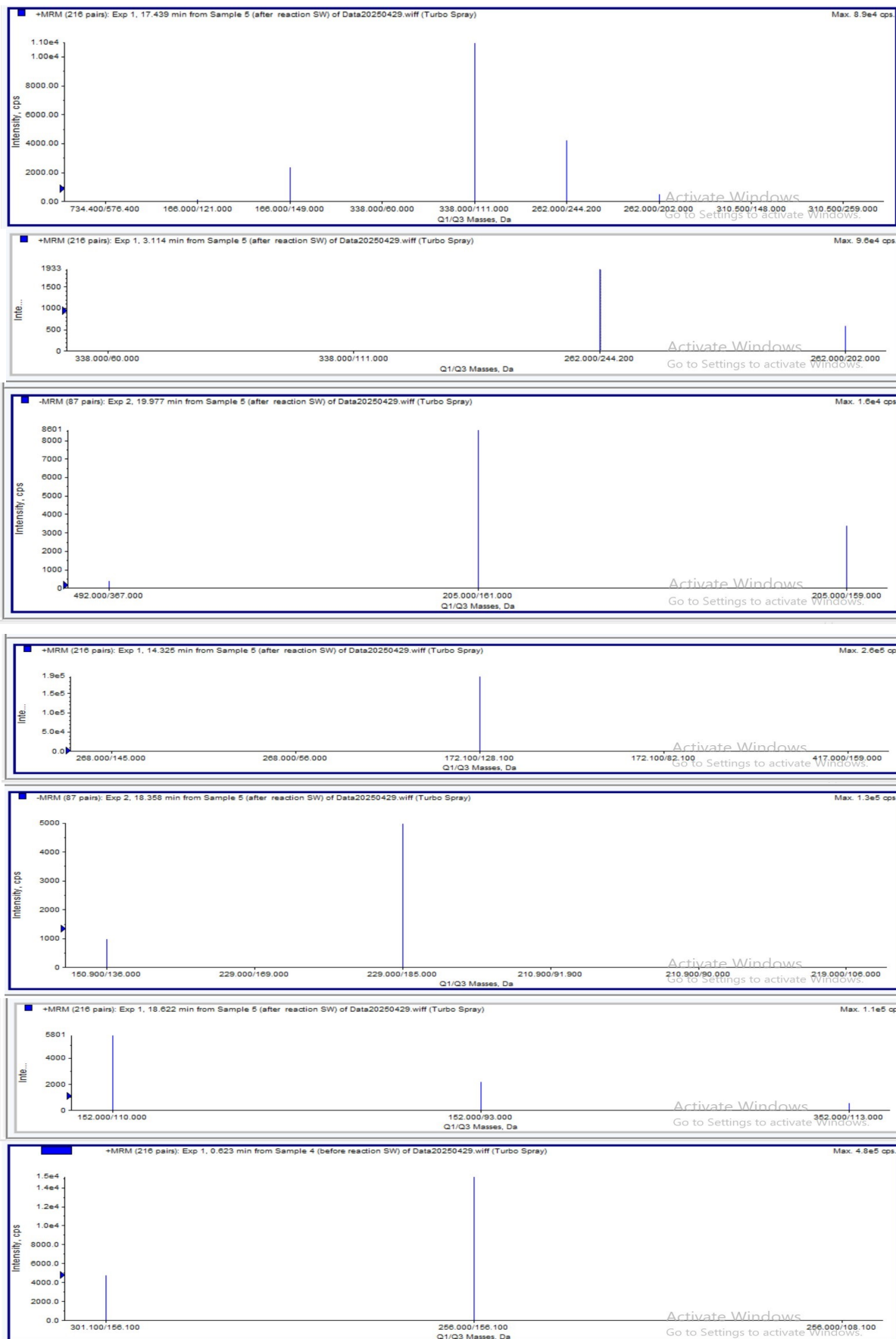
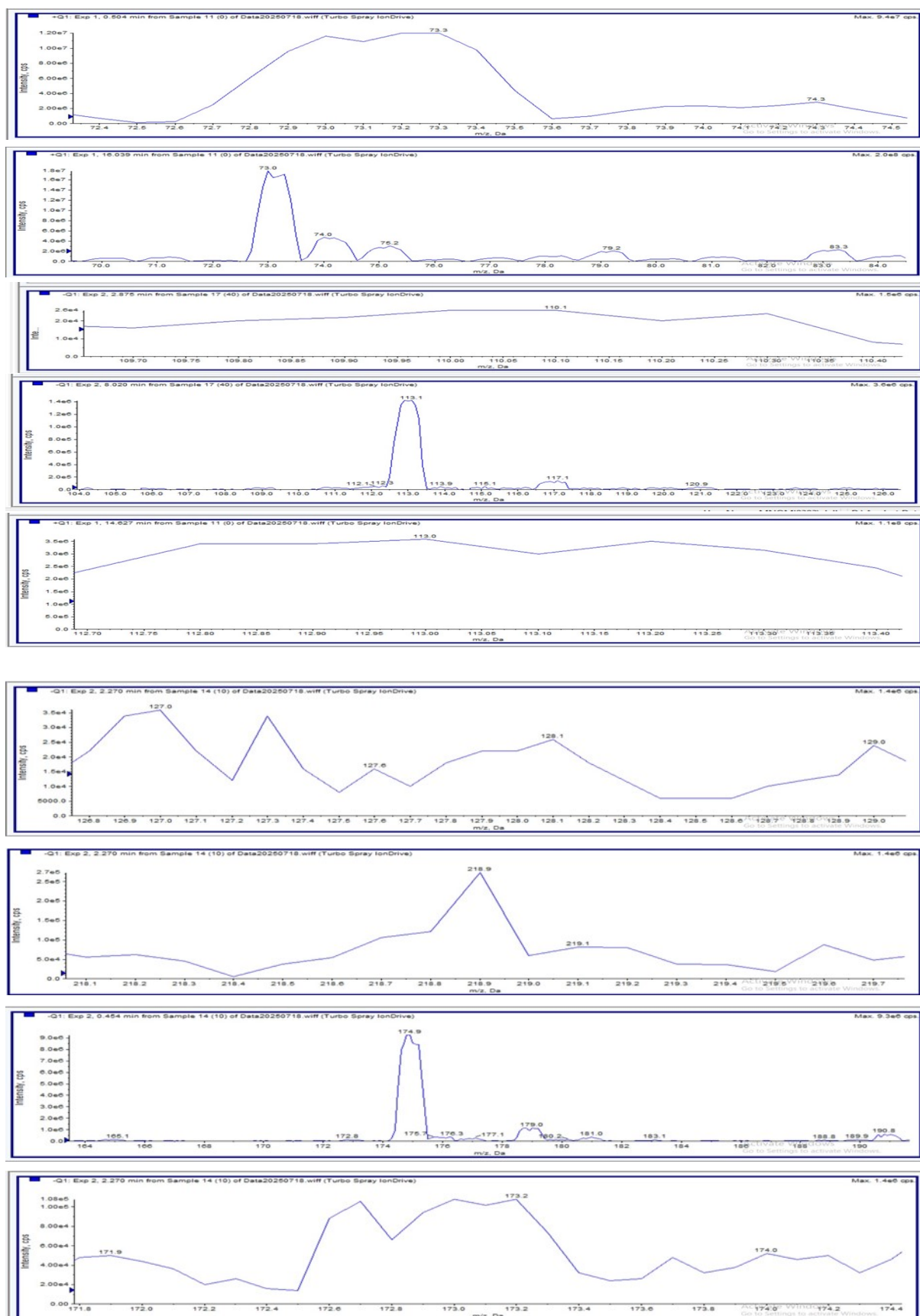
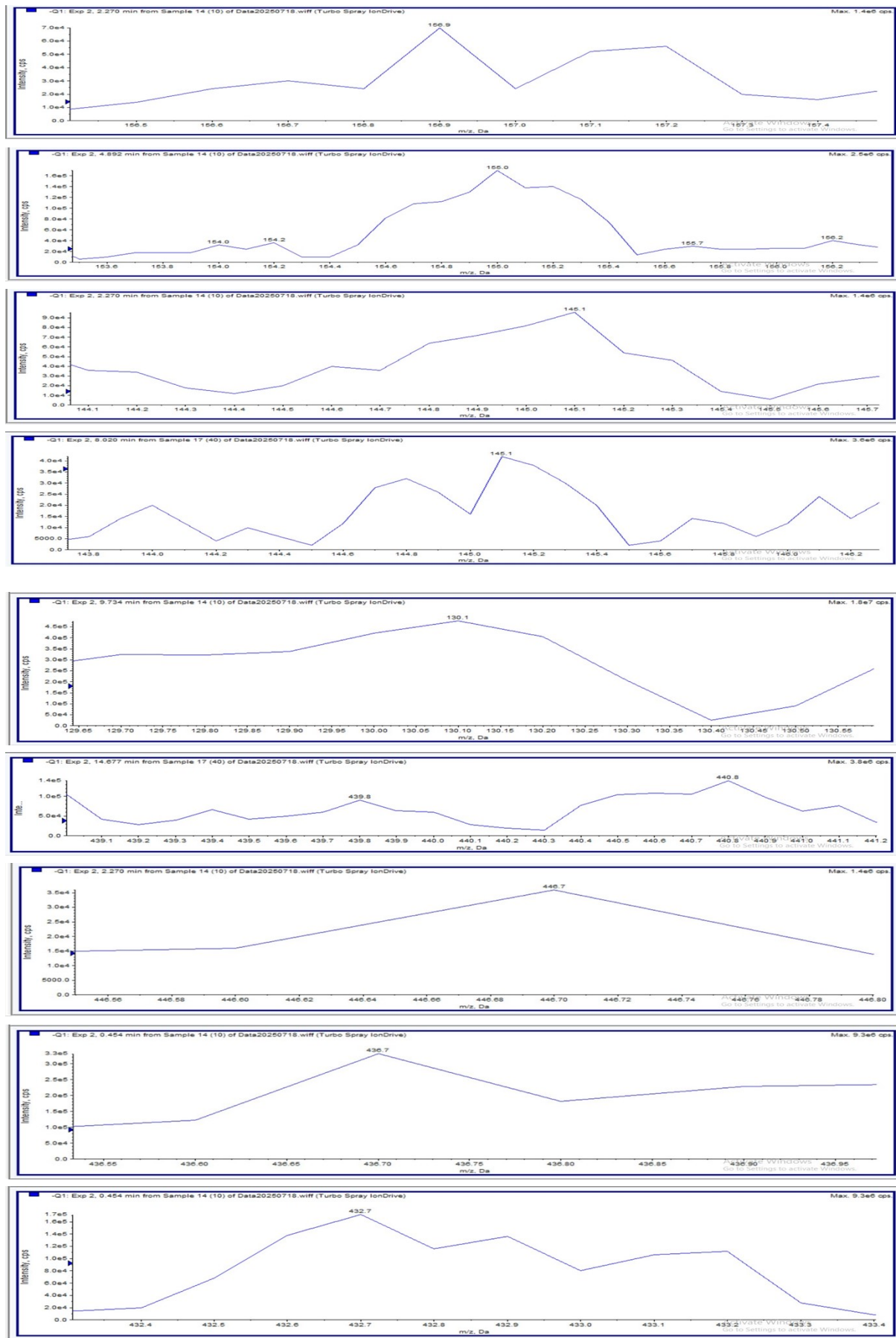
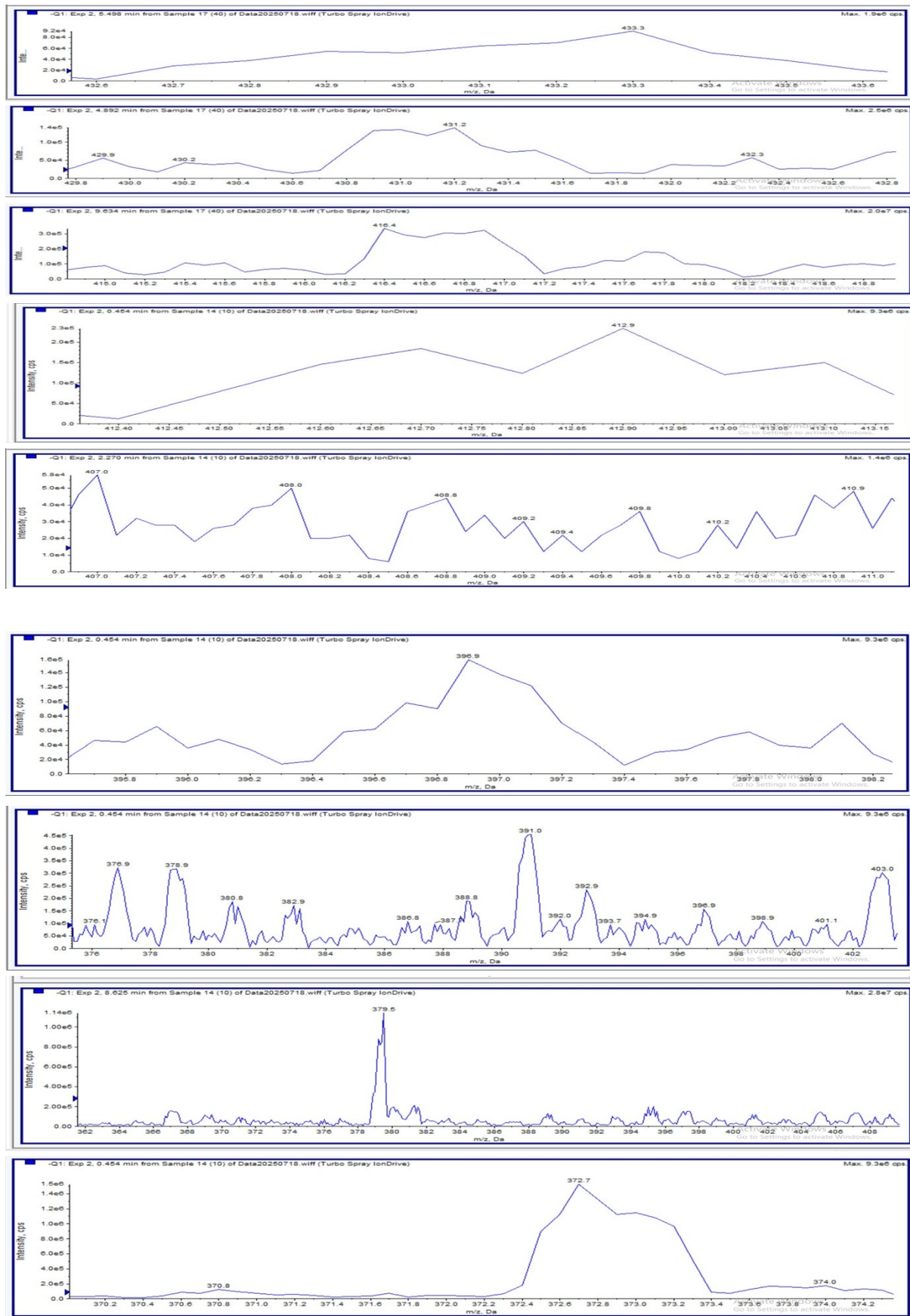
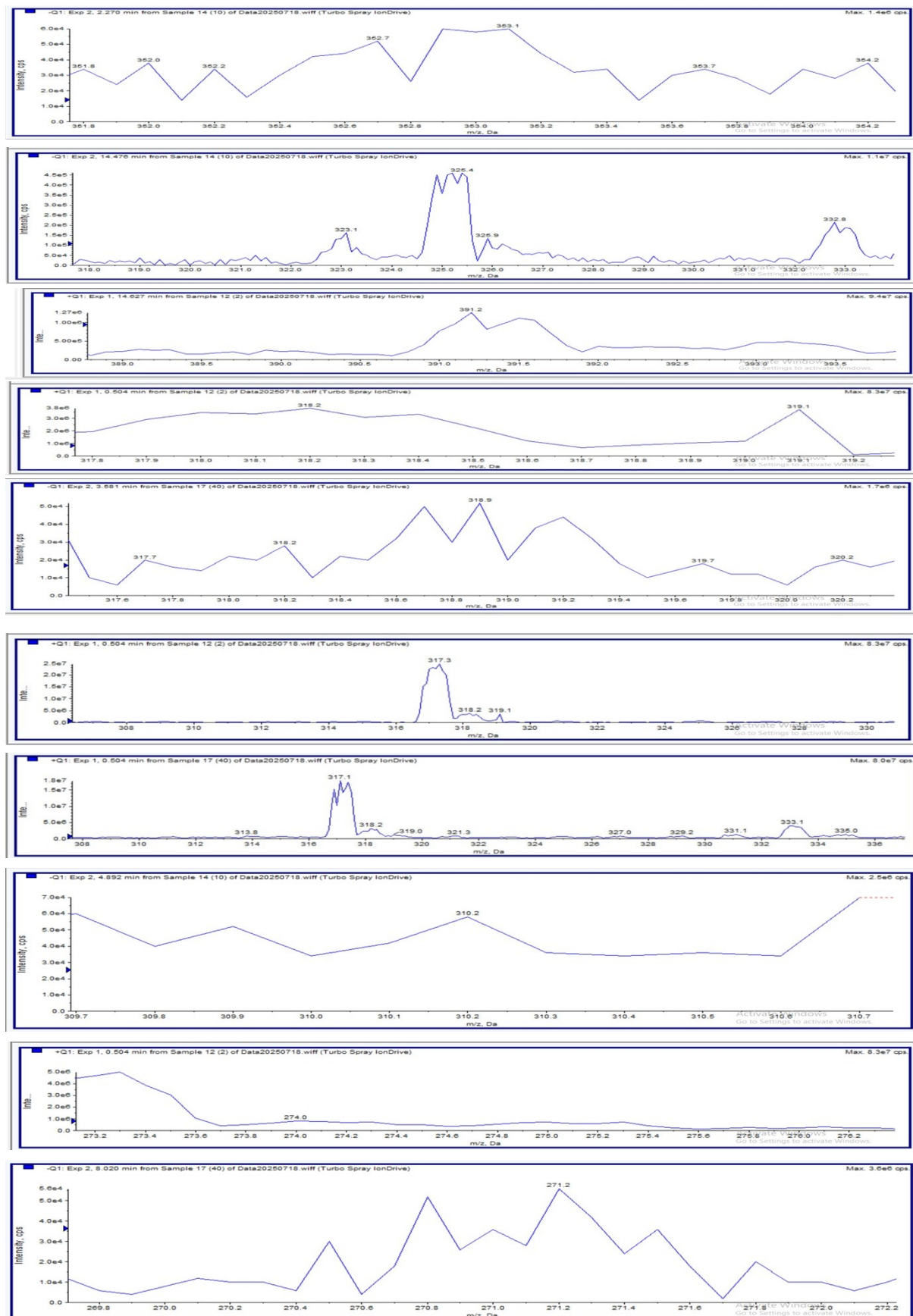


Figure S7: OTC intermediates (After reaction)









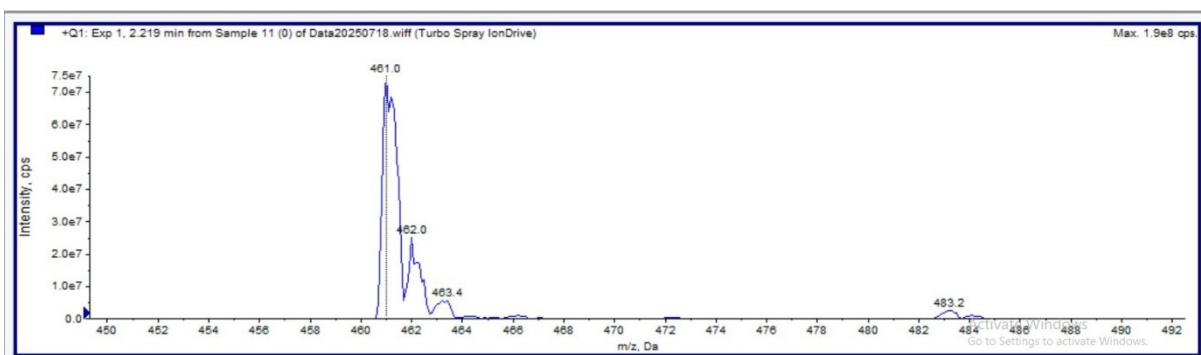
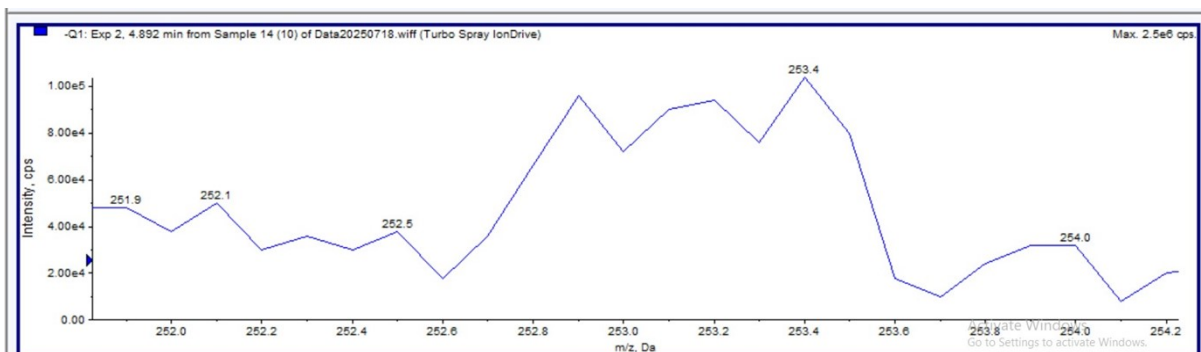
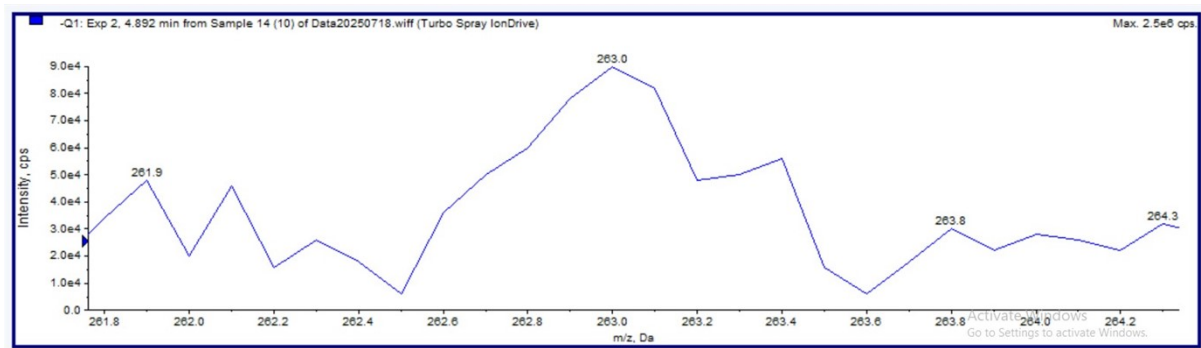


**Fig. S8:** Adsorption of OTC over 2.5%Ni/Fe-C-700°C

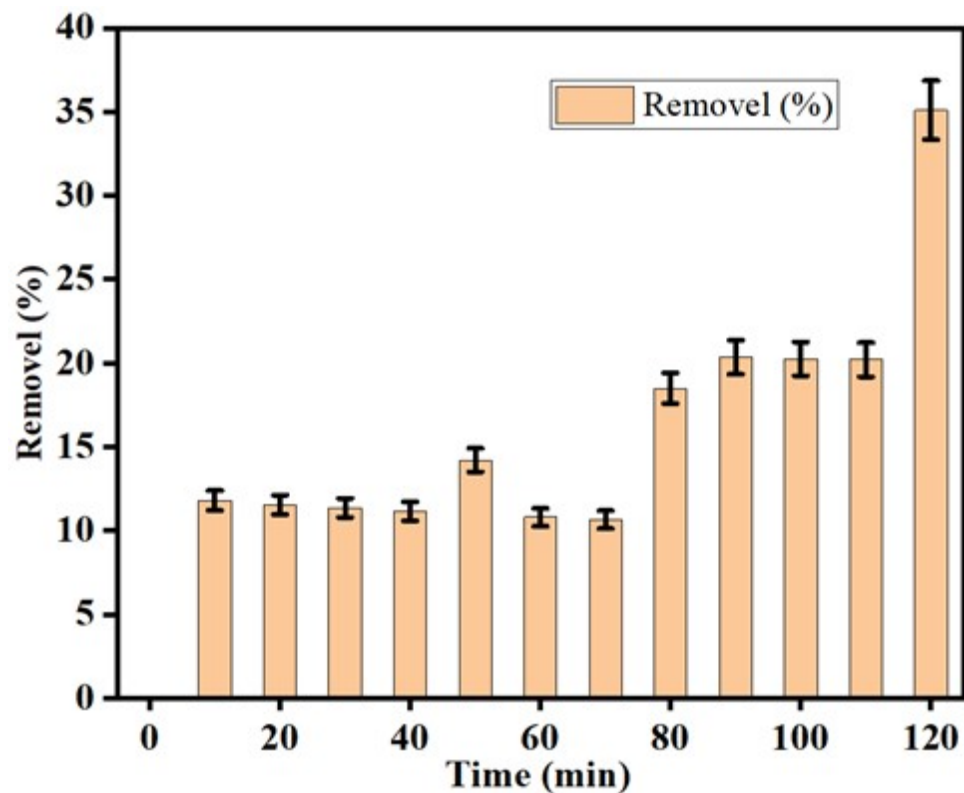


**Table S1.** Raw Partially reduced iron XRF results

Analyte	Calibration Status	Compound Formula	Concentration	Unit
Mg	Calibrated	MgO	1.103	%
Al	Calibrated	Al <sub>2</sub> O <sub>3</sub>	1.348	%
Si	Calibrated	SiO <sub>2</sub>	16.904	%
P	Calibrated	P <sub>2</sub> O <sub>5</sub>	0.673	%
S	Calibrated	SO <sub>3</sub>	0.821	%
Cl	Calibrated	Cl	0.099	%
K	Calibrated	K <sub>2</sub> O	0.087	%
Ca	Calibrated	CaO	58.312	%
Ti	Calibrated	TiO <sub>2</sub>	2.260	%
V	Calibrated	V <sub>2</sub> O <sub>5</sub>	0.000	%
Cr	Calibrated	Cr <sub>2</sub> O <sub>3</sub>	3.634	%
Mn	Calibrated	MnO	13.084	%
Fe	Calibrated	Fe <sub>2</sub> O <sub>3</sub>	0.858	%
Co	Calibrated	Co <sub>3</sub> O <sub>4</sub>	0.091	%
Sr	Calibrated	SrO	0.065	%
Nb	Calibrated	Nb <sub>2</sub> O <sub>5</sub>	0.035	%
Ba	Calibrated	BaO	0.077	%
Ce	Calibrated	CeO <sub>2</sub>	0.550	%
<b>Zr</b>	<b>Alternative</b>	<b>ZrO<sub>2</sub></b>	<b>0.000</b>	<b>%</b>

---

**Table S2.** Real Mariculture wastewater characterization

Sr.N O	Characterizations	Before reaction	After reaction
01	pH	7.9	6.19
02	TOC	120 ppm	30 ppm
03	BOD	80 ppm	20 ppm
04	DO	5 ppm	8 ppm
05	COD		
06	Turbidity	30 NTU	5 NTU
07	Suspended solids	250 mg/L	48 mg/L
08	Ammonia nitrogen (NH3-N)	7.06 mg/L	0.86 mg/L

**Table S3:** Organic Pharmaceuticals Detected in Wastewater Before Treatment

Pollutant Type	Pollutant Name	Highest Intensity (cps)	Key MRM Transition (Q1/Q3)
Endocrine Disruptors	Bisphenol AF (BPAF)	$2.4 \times 10^4$	335.000/265.000
Ketones	Acetophenones	$1.3 \times 10^5$	268.300/152.000
Pharmaceuticals	17 $\alpha$ -Ethinylestradiol (EE2)	$3.6 \times 10^5$	293.000/221.000
	Amoxicillin	$1.8 \times 10^6$	420.000/342.000
	Carbamazepine	$1.8 \times 10^3$	237.000/194.000
	Ceftizoxime	$6.0 \times 10^5$	460.300/361.200
	Clenbuterol	$1.8 \times 10^6$	277.000/203.000
	Diclofenac	$1.5 \times 10^4$	294.000/260.000
	Famotidine	$3.6 \times 10^3$	166.000/121.000

Pollutant Type	Pollutant Name	Highest Intensity (cps)	Key MRM Transition (Q1/Q3)
	Fenoprofen	$4.7 \times 10^4$	241.000/93.000
	Flumequine	$1.5 \times 10^3$	262.200/244.000
	Ibuprofen	$3.0 \times 10^5$	296.200/212.900
	Lincomycin	$1.8 \times 10^3$	362.200/261.200
	Metronidazole	$8.9 \times 10^3$	172.100/128.100
	Naproxen	$1.3 \times 10^5$	228.000/169.000
	Paracetamol	$4.7 \times 10^4$	152.000/110.000
	Sulfathiazole	$4.8 \times 10^5$	266.000/156.100

**Table S4: Organic Pharmaceuticals Detected in Wastewater After Catalytic Treatment**

Pollutant Type	Pollutant Name	Highest Intensity (cps)	Key MRM Transition (Q1/Q3)
Endocrine Disruptors	Bisphenol AF (BPAF)	$2.3 \times 10^3$	335.000/266.000
Ketones	Acetophenones	$9.1 \times 10^4$	274.100/256.000
Pharmaceuticals	Amoxicillin	ND*	420.000/342.000
	Carbamazepine	$1.7 \times 10^3$	237.000/194.000
	Ceftizoxime	$2.0 \times 10^5$	274.100/102.000
	Clenbuterol	$1.3 \times 10^3$	277.000/203.000
	Ibuprofen	$1.0 \times 10^4$	296.200/212.900
	Metronidazole	$8.9 \times 10^3$	172.100/128.100

Pollutant Type	Pollutant Name	Highest Intensity (cps)	Key MRM Transition (Q1/Q3)
	Naproxen	$5.2 \times 10^3$	228.000/168.000
	Paracetamol	$5.8 \times 10^3$	152.000/110.000
	Sulfathiazole	$9.8 \times 10^0$	256.000/156.100

**Table S5: Adsorption energies and adsorption distances calculation**

(Ozone over 2.5%Ni/Fe-C-700°C's adsorption models)

Models	E catalyst (kcal/mol)	ozone (kcal/mol)	E(adsorption system) (kcal/mol)	Eads (kcal/mol)	Eads (eV)	Adsorption Distance
<b>Fe-O</b>	143.945239	32.873527	31.284	-145.5348	-6.3105	6.235
<b>Ni-O</b>	143.945239	32.873527	31.293	-145.5258	-6.3101	6.576
<b>COOH</b>	143.945239	32.873527	31.322	-145.4968	-6.3085	6.737
<b>OH</b>	143.945239	32.873527	31.319	-145.4998	-6.3086	3.915
<b>C=O</b>	143.945239	32.873527	31.400	-145.4188	-6.3051	4.839
<b>C≡O</b>	143.945239	32.873527	31.294	-145.5248	-6.3101	4.889
<b>Defects</b>	143.945239	32.873527	31.298	-145.5208	-6.3099	3.628
<b>Edges</b>	143.945239	32.873527	31.237	-145.5818	-6.3134	5.461

**Table S6: OTC Fukui Indices for Electrophilic Attack (Fukui (-))**

Atom	Mulliken Charge	Hirshfeld Charge
O (1)	0.008	0.013
O (2)	-0.016	-0.002
O (3)	0.008	0.008

<b>Atom</b>	<b>Mulliken Charge</b>	<b>Hirshfeld Charge</b>
O (4)	0.026	0.020
O (5)	0.027	0.025
O (6)	0.018	0.015
O (7)	0.045	0.037
O (8)	0.004	0.007
O (9)	0.024	0.023
N (10)	0.196	0.222
N (11)	0.010	0.016
C (12)	-0.013	-0.002
C (13)	-0.003	0.002
C (14)	-0.006	0.003
C (15)	-0.016	-0.004
C (16)	-0.046	0.022
C (17)	-0.007	0.001
C (18)	-0.005	-0.005
C (19)	-0.006	-0.004
C (20)	0.016	0.009
C (21)	-0.003	-0.002
C (22)	-0.014	-0.001
C (23)	0.011	0.011

<b>Atom</b>	<b>Mulliken Charge</b>	<b>Hirshfeld Charge</b>
C (24)	-0.001	0.002
C (25)	-0.003	0.004
C (26)	-0.005	-0.003
C (27)	0.002	0.006
C (28)	-0.049	0.040
C (29)	-0.049	0.042
C (30)	0.005	0.006
C (31)	0.007	0.003
C (32)	0.007	0.015
C (33)	0.005	0.011
H (34)	0.017	0.005
H (35)	0.009	0.002
H (36)	0.016	0.005
H (37)	0.090	0.051
H (38)	0.007	0.004
H (39)	0.018	0.010
H (40)	0.009	0.005
H (41)	0.011	0.008
H (42)	0.021	0.013
H (43)	0.006	0.003

<b>Atom</b>	<b>Mulliken Charge</b>	<b>Hirshfeld Charge</b>
H (44)	0.013	0.006
H (45)	0.072	0.038
H (46)	0.112	0.069
H (47)	0.066	0.033
H (48)	0.113	0.071
H (49)	0.071	0.041
H (50)	0.069	0.035
H (51)	0.012	0.011
H (52)	0.005	0.004
H (53)	0.020	0.010
H (54)	0.019	0.009
H (55)	0.009	0.007
H (56)	0.025	0.015
H (57)	0.010	0.007

**Table S7:** OTC Fukui Indices for Nucleophilic Attack (Fukui (+))

<b>Atom</b>	<b>Mulliken Charge</b>	<b>Hirshfeld Charge</b>
O (1)	0.014	0.016
O (2)	0.028	0.027
O (3)	0.015	0.015
O (4)	0.118	0.111

<b>Atom</b>	<b>Mulliken Charge</b>	<b>Hirshfeld Charge</b>
O (5)	0.029	0.030
O (6)	0.041	0.034
O (7)	0.065	0.059
O (8)	0.010	0.016
O (9)	0.042	0.036
N (10)	-0.010	-0.001
N (11)	0.008	0.012
C (12)	-0.009	0.003
C (13)	-0.012	0.004
C (14)	0.004	-0.001
C (15)	-0.018	0.014
C (16)	-0.004	0.004
C (17)	-0.008	0.003
C (18)	-0.007	0.008
C (19)	0.106	0.104
C (20)	0.024	0.024
C (21)	0.013	0.012
C (22)	0.019	0.026
C (23)	0.036	0.040
C (24)	0.031	0.032

<b>Atom</b>	<b>Mulliken Charge</b>	<b>Hirshfeld Charge</b>
C (25)	-0.007	0.005
C (26)	-0.007	0.003
C (27)	0.007	0.019
C (28)	-0.013	0.005
C (29)	-0.017	0.005
C (30)	0.019	0.017
C (31)	0.004	0.006
C (32)	0.023	0.037
C (33)	0.010	0.022
H (34)	0.025	0.010
H (35)	0.023	0.010
H (36)	0.008	0.003
H (37)	0.027	0.014
H37	0.027	0.014
H38	0.021	0.010
H39	0.025	0.013
H40	0.004	0.003
H41	0.014	0.010
H42	0.019	0.013
H43	0.014	0.010

<b>Atom</b>	<b>Mulliken Charge</b>	<b>Hirshfeld Charge</b>
H44	0.030	0.015
H45	-0.001	0.001
H46	0.020	0.010
H47	0.027	0.014
H48	0.021	0.010
H49	0.004	0.004
H50	0.027	0.014
H51	0.012	0.011
H52	0.008	0.012
H53	0.039	0.021
H54	0.035	0.017
H55	-0.004	0.001
H56	0.028	0.016
H57	0.019	0.015

**Table S8:** OTC Fukui Indices for Radical attack (Fukui (0))

<b>Atom</b>	<b>Mulliken Charge</b>	<b>Hirshfeld Charge</b>
<b>O (1)</b>	0.011	0.015
<b>O (2)</b>	0.006	0.012
<b>O (3)</b>	0.011	0.012
<b>O (4)</b>	0.072	0.065

<b>Atom</b>	<b>Mulliken Charge</b>	<b>Hirshfeld Charge</b>
<b>O (5)</b>	0.028	0.028
<b>O (6)</b>	0.029	0.025
<b>O (7)</b>	0.055	0.048
O (8)	0.007	0.011
O (9)	0.033	0.030
N (10)	0.093	0.111
N (11)	0.009	0.014
C (12)	-0.011	0.000
C (13)	-0.007	0.003
C (14)	-0.001	0.001
C (15)	-0.017	0.005
C (16)	-0.025	0.013
C (17)	-0.008	0.002
C (18)	-0.006	0.002
C (19)	0.050	0.050
C (20)	0.020	0.016
C (21)	0.005	0.005
C (22)	0.003	0.012
C (23)	0.024	0.025
C (24)	0.015	0.017

<b>Atom</b>	<b>Mulliken Charge</b>	<b>Hirshfeld Charge</b>
C (25)	-0.005	0.005
C (26)	-0.006	0.000
C (27)	0.005	0.013
C (28)	-0.031	0.022
C (29)	-0.033	0.023
C (30)	0.012	0.011
C (31)	0.005	0.004
C (32)	0.015	0.026
C (33)	0.008	0.016
H (34)	0.021	0.008
H (35)	0.016	0.006
H (36)	0.012	0.004
H (37)	0.059	0.032
H (38)	0.014	0.007
H (39)	0.022	0.011

H40	0.006	0.004
H41	0.012	0.009
H42	0.020	0.013
H43	0.010	0.006
H44	0.021	0.010

Atom	Mulliken Charge	Hirshfeld Charge
H45	0.036	0.019
H46	0.066	0.039
H47	0.046	0.023
H48	0.067	0.040
H49	0.038	0.022
H50	0.048	0.024
H51	0.012	0.011
H52	0.006	0.008
H53	0.030	0.016
H54	0.027	0.013
H55	0.002	0.004
H56	0.026	0.016
H57	0.015	0.011

**Table S9:** OTC degradation efficiency with other studies.

Number of Studies	Pollutant load	Catalyst dosage	Removal rate (%)	Ozone concentration/PMS	References
This work	10 mg/L	0.1 g/L	96.7	6.5	This work
1	20 mg/L	0.2 g/L	100	0.2mM	[9]
2	20 mg/L	0.4 g/L	92.81	Adsorption	[10]
3	10.68 mg/L	0.46 g/L	99.52	0.21 g/L	[11]
4	270 mg/L	0.5 g/L	89.5	10 mg/L	[12]
5	5 mg/L	0.25 g/L	89.5	adsorption	[13]
6	10 mg/L	0.25 g/L	84.5	Photocatalytic reaction	[14]
7	10 mg/L	1 g/L	85.9	80 mM (PMS)	[15]
8	20 mg/L	0.20g/100mL	94.38	Photocatalytic reaction	[16]
9	10 mg/L	0.1 g/L	99.9	1 mM (PMS)	[17]

10	5 mg/L	0.2 g/L	97.9	Photocatalytic reaction	[18]
11	50 mM	0.1 g/L	90.92	5 mM	[19]
12	30 mg/L	0.01 mole/L	96	Photo-Fenton degradation	[20]

**Table S10: Life-cycle inventory (LCI) based attributional cradle-to-grave LCA calculations**

Metric	Result per 0.5 kg catalyst	Greener ?	Why It's Greener
<b>Avoided Burden - Coconut Shell</b>	0.30 kg CO <sub>2</sub> -eq saved	Yes	Diverts agricultural waste from landfill, reducing methane emissions
<b>Avoided Burden - Iron Fines</b>	0.01 kg CO <sub>2</sub> -eq saved	Yes	Utilizes industrial by-products that would otherwise go to waste
<b>Toxicity Impact (Ni)</b>	$1.55 \times 10^{-6}$ CTUh	Yes	Nickel toxicity impact is negligible (extremely low)
<b>Circularity (4 cycles)</b>	4.4% circular	Yes	Enables multiple reuse cycles, reducing virgin material demand
<b>Regeneration Credit</b>	3.27 kg CO <sub>2</sub> -eq saved	Yes	Regeneration uses 81% less CO <sub>2</sub> than making a new catalyst
<b>Net Environmental Benefit</b>	<b>3.58 kg CO<sub>2</sub>-eq net saved</b>	Yes	<b>Overall significant carbon reduction + waste valorization</b>

### Life-cycle inventory (LCI) based attributional cradle-to-grave LCA

#### 1 Avoided-burden credit for waste utilization

##### 1. 2 Coconut Shell Residue (Pyrolysed to Biochar)

- **Mass (m\_CNR):** 0.30 kg (60% of the 0.5 kg composite)
- **Disposal CF (Landfill, GWP):** 1.0 kg CO<sub>2</sub>-eq kg<sup>-1</sup> (for wet biomass, IPCC 2019)
- **Avoided GWP Impact:**

$$0.30 \text{ kg} \times 1.0 \text{ kg CO}_2\text{-eq kg}^{-1} = 0.30 \text{ kg CO}_2\text{-eq}$$

##### 1.3 Partially-Reduced Iron-Ore Fines (RI)

- **Mass (m\_RI):** 0.20 kg (40% of the 0.5 kg composite)

- **Disposal CF (Landfill, GWP):**  $0.05 \text{ kg CO}_2\text{-eq kg}^{-1}$  (for inert mineral waste)
- **Avoided GWP Impact:**

$$0.20 \text{ kg} \times 0.05 \text{ kg CO}_2\text{-eq kg}^{-1} = 0.01 \text{ kg CO}_2\text{-eq}$$

## 2. Toxicity increment from impurities in waste feedstock (Based on EDS)

### EDS Analysis of 0.5 kg Catalyst:

- Nickel (Ni):  $2.38\% = 0.0119 \text{ kg}$
- Iron (Fe):  $0.27\% = 0.00135 \text{ kg}$
- Carbon (C):  $6.96\% = 0.0348 \text{ kg}$  (non-toxic)
- Oxygen (O):  $36.14\% = 0.1807 \text{ kg}$  (non-toxic)

### USEtox Factors (Human Toxicity, Soil Emission):

- Ni:  $1.3 \times 10^{-4} \text{ CTUh kg}^{-1}$
- Fe: Considered non-toxic in LCA ( $\text{CF} \approx 0$ )

### Toxicity Calculation:

- Ni Impact =  $0.0119 \text{ kg} \times 1.3 \times 10^{-4} \text{ CTUh kg}^{-1} = 1.55 \times 10^{-6} \text{ CTUh}$
- Fe Impact =  $0.00135 \text{ kg} \times 0 \text{ CTUh kg}^{-1} = 0 \text{ CTUh}$
- **Total Impact =  $1.55 \times 10^{-6} \text{ CTUh}$**

### Why Only Ni Matters:

- Ni has a high concentration (2.38%) and significant toxicity
- Fe is an essential nutrient, non-toxic in LCA models
- C and O are non-toxic elements
- No other metals detected in EDS analysis

**Final: Toxicity Increment =  $1.55 \times 10^{-6} \text{ CTUh per m}^3$  wastewater.**

## 3. Resource Efficiency & Circular Metrics (Catalyst Life Cycle)

### Basic Formula:

$$\text{MCI} = \text{Waste fraction} \times (\text{Waste fraction})^{\wedge} (\text{cycles}-1)$$

### Where:

- Waste fraction = 45.75% = 0.4575
- Cycles = 4

### Calculation:

$$\begin{aligned} \text{MCI} &= 0.4575 \times (0.4575)^3 \\ &= 0.4575 \times 0.4575 \times 0.4575 \times 0.4575 \\ &= 0.044 \text{ (or 4.4\%)} \end{aligned}$$

### Cycle-by-cycle breakdown:

- After 1 cycle: 45.75% circular
- After 2 cycles: 20.9% circular
- After 3 cycles: 9.6% circular
- After 4 cycles: **4.4% circular**

## 4. Regeneration Efficiency and Impact (Catalyst Discharge/End-of-Life)

### Given Data:

- Fresh catalyst impact:  $2.1 \text{ kg CO}_2\text{-eq/kg}$
- Regenerated catalyst impact:  $0.4 \text{ kg CO}_2\text{-eq/kg}$
- Cycles: 5

- Recovery efficiency: 95% per cycle

**Calculation Formula:**

$$\text{Credit} = (\text{Impact}_\text{fresh} - \text{Impact}_\text{reg}) \times \text{Effective Cycles}$$

**Step 1: Calculate Savings Per Cycle**

$$2.1 - 0.4 = 1.7 \text{ kg CO}_2\text{-eq/kg per regeneration}$$

**Step 2: Calculate Effective Cycles (Accounting for 5% Loss)**

$$\text{After 5 cycles: } 0.95^5 = 0.77 \text{ (77% mass remains)}$$

$$\text{Effective cycles} = 5 \times 0.77 = 3.85 \text{ cycles}$$

**Step 3: Calculate Total Credit**

$$\text{Credit} = 1.7 \times 3.85 = 6.55 \text{ kg CO}_2\text{-eq/kg catalyst}$$

**Step 4: Apply to Functional Unit (0.5 kg catalyst)**

$$6.55 \times 0.5 = 3.27 \text{ kg CO}_2\text{-eq saved}$$

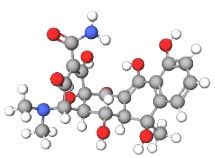
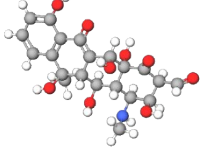
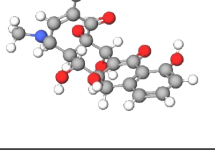
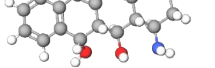
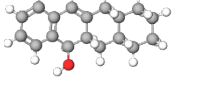
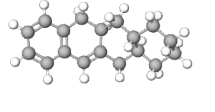
**Final Result:**

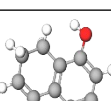
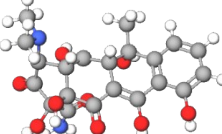
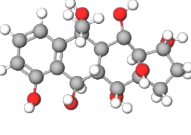
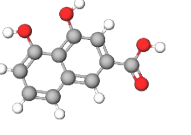
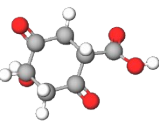
3.27 kg CO<sub>2</sub>-eq saved per 0.5 kg catalyst over 5 regeneration cycles.

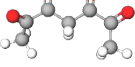
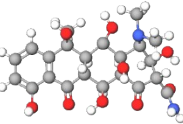
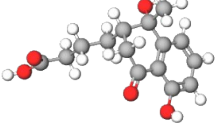
**Table S11: Comprehensive comparison of 2.5%Ni/Fe-C-700°C with other catalysts based on other factors**

Sr. No	Material	OTC concentration	Cost estimation	Removal efficiency	Ozone consumption	References
01	Z5Å-Co-Fe/O <sub>3</sub>	OTC in a real matrix	Not report	95 % (15 min, pH 6)	1.6 mg min <sup>-1</sup>	[21]
02	Mn1-Mg2/Al <sub>2</sub> O <sub>3</sub>	OTC hydrochloride	not reported	82.5–89.5 % OTC,	not reported	[12]
03	Mn1-Mg2/Al <sub>2</sub> O <sub>3</sub>	OTC hydrochloride	not reported	82.5–89.5 % OTC	not reported	[12]
04	CaO <sub>2</sub> /O <sub>3</sub>	WWTP sludge	not reported	90 % VS,	CaO <sub>2</sub> /O <sub>3</sub>	[22]
05	Bi <sub>2</sub> S <sub>3</sub> @NH <sub>2</sub> -MIL-125(Ti)	10 mg/L tocilizumab		176 % TOC (15 min)	5 L h <sup>-1</sup>	[11]
07	SCBW-10 (SCB/WS <sub>2</sub> )	5 mg L <sup>-1</sup> OTC	not reported	92.7 % (180 min, pH 7)	none (photocatalysis)	[23]
09	pmSA800	20 mg/L	1.60 USD	0.2mM	20 mg/L	[23]
08	<b>2.5%Ni/Fe-C-700°C</b>	<b>10 mg/L</b>	<b>1.547 USD (waste-based)</b>	<b>96.74%</b>	<b>5.5± 0.5 mg/L</b>	<b>This study</b>

**Table S12: Toxicity assessment of all intermediates of OTC over 2.5%Ni/Fe-C-700°C/O<sub>3</sub>**

Sr. No	Intermediates	Bioconcentration_	Daphnia magna LC50_(48_hr)	Developmental	Mutagenicity
OTC		2.78	11.98	Developmental toxicant	Mutagenicity Positive
P1		2.78	11.98	Developmental toxicant	Mutagenicity Positive
P2		N/A	N/A	N/A	N/A
P3		N/A	N/A	N/A	N/A
P4		7.34	3.25	Developmental toxicant	Mutagenicity Negative
P5		76.81	2.62	Developmental toxicant	Mutagenicity Positive
P6		810.47	0.20	Developmental toxicant	Mutagenicity Positive

P7		3.20	227.64	Developmental toxicant	Mutagenicity Negative
P8		5.05	11.58	Developmental toxicant	Mutagenicity Negative
P9		17.25	5.39	Developmental toxicant	Mutagenicity Positive
R1		N/A	N/A	N/A	N/A
R2		N/A	N/A	Developmental toxicant	Mutagenicity Positive
R3		2.49	72.85	Developmental toxicant	Mutagenicity Negative
R4		17.58	4.44	Developmental toxicant	Mutagenicity Negative
R5		5.91E-02	681.86	Developmental NON-toxicant	Mutagenicity Negative

R6a		0.19	218.03	Developmental toxicant	Mutagenicity Negative
R6b		3.59E-02	274.64	Developmental toxicant	Mutagenicity Negative
T1		4.60	68.65	Developmental toxicant	Mutagenicity Positive
T2		N/A	N/A	Developmental toxicant	N/A
T3		2.30	186.00	Developmental toxicant	Mutagenicity Negative

## References

1. Heijungs, R. and J.B. Guinée, *Allocation and ‘what-if’ scenarios in life cycle assessment of waste management systems*. Waste Management, 2007. **27**(8): p. 997-1005.
2. Liu, J., et al., *Impact of recycling effect in comparative life cycle assessment for materials selection - A case study of light-weighting vehicles*. Journal of Cleaner Production, 2022. **349**: p. 131317.
3. Belyanovskaya, A.I., et al., *The Innovation of the characterisation factor estimation for LCA in the USETOX model*. Journal of Cleaner Production, 2020. **270**: p. 122432.
4. Gandhi, N., et al., *Implications of considering metal bioavailability in estimates of freshwater ecotoxicity: examination of two case studies*. The International Journal of Life Cycle Assessment, 2011. **16**(8): p. 774-787.
5. Bracquené, E., W. Dewulf, and J.R. Duflou, *Measuring the performance of more circular complex product supply chains*. Resources, Conservation and Recycling, 2020. **154**: p. 104608.
6. Tashkeel, R., et al., *Cost-Normalized Circular Economy Indicator and Its Application to Post-Consumer Plastic Packaging Waste*. LID - 10.3390/polym13203456 [doi] LID - 3456. (2073-4360 (Electronic)).
7. Rocchi, L., et al., *Measuring circularity: an application of modified Material Circularity Indicator to agricultural systems*. Agricultural and Food Economics, 2021. **9**(1): p. 9.
8. Astudillo, M.F., G. Thalwitz, and F. Vollrath, *Life cycle assessment of Indian silk*. Journal of Cleaner Production, 2014. **81**: p. 158-167.
9. Lin, T., et al., *Direct generation of high-valent iron-oxo species to eliminate oxytetracycline at circumneutral pH via paper mill sludge ash activating peroxyomonosulfate*. Chemical Engineering Journal, 2024. **484**: p. 150021.
10. Pang, W., et al., *Organic ligands modulation of Ti-based hierarchical MOFs to improve visible-light-driven catalytic degradation properties for tetracycline antibiotics*. Separation and Purification Technology, 2025. **361**: p. 131600.
11. Sun, L., et al., *Water flow-driven N-CQDS/MoS<sub>2</sub> piezoelectric-photocatalytic percarbonate degradation of oxytetracycline: Response surface modeling and mechanistic analysis*. Journal of Environmental Chemical Engineering, 2025. **13**(5): p. 117563.
12. Xing, B., et al., *Regulating surface acid-base properties of Mn-Mg/Al<sub>2</sub>O<sub>3</sub> for the enhanced catalytic ozonation of oxytetracycline hydrochloride degradation*. Journal of Environmental Chemical Engineering, 2025. **13**(2): p. 115740.
13. Zhang, J., et al., *Construction of Fe-MOF/ZIF derivative C1M5 for efficient activation*

*of PS-degraded OTC by adsorption-oxidation synergy: Performance and potential activation mechanism.* Separation and Purification Technology, 2025. **353**: p. 128595.

- 14. Vargas-Bustamante, J., et al., *Comparative study of (NiFe<sub>2</sub>O<sub>4</sub>) photocatalysts for oxytetracycline degradation: Effect of synthesis method on performance stability.* Materials Chemistry and Physics, 2025. **346**: p. 131242.
- 15. Zhao, Q., et al., *Insight into the facet-dependent activity of MnFe<sub>2</sub>O<sub>4</sub> in H<sub>2</sub>O<sub>2</sub> activation for efficient oxytetracycline degradation.* Chemical Engineering Journal, 2025. **520**: p. 165974.
- 16. Deng, C., et al., *Enhanced visible light photocatalytic degradation of oxytetracycline hydrochloride using heterojunction BiOBr/TiO<sub>2</sub> composites.* Applied Surface Science, 2025. **710**: p. 163945.
- 17. Kumari, M. and M. Pulimi, *Sulfate radical-based degradation of oxytetracycline with CuO/UiO-66 doped hydrochar: Mechanistic insights and toxicity studies.* Colloids and Surfaces A: Physicochemical and Engineering Aspects, 2025. **718**: p. 136869.
- 18. Khurshid, H., et al., *Engineering multi-interface Co/Cu co-doped CdS@PCN hybrid architectures for use as high-efficiency visible light driven photocatalysis for the degradation of oxytetracycline.* Applied Surface Science Advances, 2025. **29**: p. 100828.
- 19. Liang, X., et al., *Magnetic recyclable Fe<sub>3</sub>O<sub>4</sub>/MoS<sub>2</sub>@Material Institute Lavoisier 100 (MIL-100(Fe)) ternary catalyst for photo-Fenton degradation of oxytetracycline hydrochloride.* Journal of Alloys and Compounds, 2025. **1038**: p. 182610.
- 20. Zheng, N., et al., *Photo-Fenton degradation of oxytetracycline by g-C<sub>3</sub>N<sub>4</sub>/CQDs/FeOCl with in-situ hydrogen peroxide production: Degradation pathway and toxicity analysis of intermediate products.* Journal of Water Process Engineering, 2025. **69**: p. 106615.
- 21. Ikhlaq, A., et al., *Novel Zeolite 5Å-Co-Fe based catalytic ozonation process for the efficient degradation of Oxytetracycline in veterinary pharmaceutical wastewater.* Cleaner Water, 2024. **1**: p. 100017.
- 22. Seid-Mohammadi, A., et al., *Efficient digestion and improvement of dewaterability of municipal wastewater treatment sludge through catalytic calcium peroxide/ozonation advanced oxidation process.* Cleaner Engineering and Technology, 2025. **27**: p. 101034.
- 23. Chauhan, S., et al., *Enhanced visible light photocatalytic degradation of oxytetracycline through sugarcane bagasse biochar supported layered WS<sub>2</sub> type-II staggered heterojunction: Towards performance, degradation pathway, toxicity, and life cycle assessment.* Environmental Research, 2025. **271**: p. 121100.